

AD-A094 219

RENSSELAER POLYTECHNIC INST TROY N Y

F/G 13/8

DEVELOPMENT AND QUALIFICATION OF METHODS FOR THE DETERMINATION --ETC(U)

SEP 80 W F SAVAGE, E F NIPPES

N00014-75-C-0944

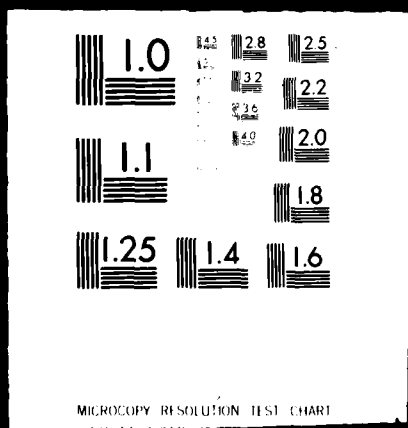
NL

UNCLASSIFIED

1 of 2  
AD-A094 219



1 OF 2  
AD A  
094219



AD A094219

LEVEL 2

TW (A)

OFFICE OF NAVAL RESEARCH  
CONTRACT NO. N00014-75-C-0944, NR 031-780

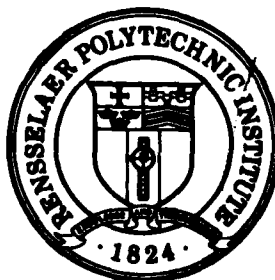
INTERIM  
✓ TECHNICAL REPORT

for the period  
July 1, 1977 to June 30, 1980

✓ "Development and Qualification of  
Methods for the Determination of Diffusible  
Hydrogen Content in Weldments"

by

W. F. Savage and E. F. Nippes



DTIC  
ELECTE  
S JAN 28 1981 D

DISTRIBUTION STATEMENT A  
Approved for public release  
Distribution Unlimited

81 1 26 210

DDC FILE COPY

UNCLASSIFIED

SECURITY CLASSIFICATION OF THIS PAGE (When Data Entered)

REPORT DOCUMENTATION PAGE		READ INSTRUCTIONS BEFORE COMPLETING FORM
1. REPORT NUMBER	2. GOVT ACCESSION NO.	3. RECIPIENT'S CATALOG NUMBER
Interim Technical Report 2	AD-A094149	
4. TITLE (and Subtitle)	5. TYPE OF REPORT & PERIOD COVERED	
DEVELOPMENT AND QUALIFICATION OF METHODS FOR THE DETERMINATION OF DIFFUSIBLE HYDROGEN CONTENTS IN WELDMENTS.	Interim July 1, 1977 - June 30, 1980	
6. AUTHOR(s)	7. CONTRACT OR GRANT NUMBER(s)	
W. F. /Savage and E. F. /Nippes	N00014-75-C-0944	
8. PERFORMING ORGANIZATION NAME AND ADDRESS	9. PROGRAM ELEMENT, PROJECT, TASK AREA & WORK UNIT NUMBERS	
Rensselaer Polytechnic Institute Troy, NY 12181	11 200 50	
10. CONTROLLING OFFICE NAME AND ADDRESS	12. REPORT DATE	
Procuring Contracting Officer Office of Naval Research Dept. of Navy, Arlington, VA 22217	September 15, 1980	
11. MONITORING AGENCY NAME & ADDRESS (if different from Controlling Office)	13. NUMBER OF PAGES	
9 Int. in technical report 2 Jul 77 - 30 Jun 80 82	15. SECURITY CLASS. (of this report)	
	UNCLASSIFIED	
16. DISTRIBUTION STATEMENT (of this Report)	15a. DECLASSIFICATION/DOWNGRADING SCHEDULE	
<div style="display: flex; justify-content: space-between;"> <div> REPRODUCTION OF PERMITTED FOR ANY PUI </div> <div style="border: 1px solid black; padding: 5px; text-align: center;"> DISTRIBUTION STATEMENT A Approved for public release Distribution Unlimited </div> <div> </div> </div>		
17. DISTRIBUTION STATEMENT (of the abstract entered in Block 20, if different from Report)		
18. SUPPLEMENTARY NOTES		
19. KEY WORDS (Continue on reverse side if necessary and identify by block number)		
WELDING HY-130 HYDROGEN BARNACLE CELL EMBRITTELEMENT SILICONE-OIL EXTRACTION METHOD MASS SPECTROMETER HYDROGEN-INDUCED CRACKING		
20. ABSTRACT (Continue on reverse side if necessary and identify by block number)		
Because a critical concentration of diffusible hydrogen must be present for hydrogen-induced cracking, it is essential to determine the amount of hydrogen introduced by various welding procedures.		

DD FORM 1 JAN 73 1473

EDITION OF 1 NOV 65 IS OBSOLETE  
S/N 0102-LF-014-6601

UNCLASSIFIED

SECURITY CLASSIFICATION OF THIS PAGE (When Data Entered)

**UNCLASSIFIED**

SECURITY CLASSIFICATION OF THIS PAGE (When Data Entered)

ont → This investigation involved the development and qualification of three methods for the determination of diffusible hydrogen content in weldments.

(1) A hot-extraction method utilizing a mass spectrometer:

If a suitable quenching procedure were developed, the mass-spectrometer extraction method could be used to measure the diffusible and total hydrogen contents of weld-metal specimens;

(2) An electrochemical technique using a modification of the Barnacle Cell:

The modified Barnacle Cell cannot be used to determine accurately the diffusible hydrogen content in weldments because accurate diffusivity values are not known, or are difficult to determine;

3. A silicone-oil extraction method developed at RPI:

This method is a reliable, rapid and inexpensive technique for the determination of diffusible-hydrogen content in weldments.

Accession For	
NTIS GRA&I	<input checked="" type="checkbox"/>
DTIC TAB	<input type="checkbox"/>
Unannounced	<input type="checkbox"/>
Justification	
By <b>Per Ltr. on file</b>	
Distribution/	
Availability Codes	
Dist	Avail and/or Special
<b>A</b>	<b>1</b>

**UNCLASSIFIED**

SECURITY CLASSIFICATION OF THIS PAGE (When Data Entered)

## TABLE OF CONTENTS

	<u>Page</u>
LIST OF TABLES .....	vi
LIST OF FIGURES .....	viii
ACKNOWLEDGEMENTS .....	x
ABSTRACT .....	xii
INTRODUCTION .....	1
OBJECT .....	5
MASS-SPECTROMETER HOT-EXTRACTION METHOD .....	7
Specimen Preparation .....	7
Apparatus .....	12
Calibration of Apparatus .....	19
Analytical Procedure .....	21
RESULTS AND DISCUSSION .....	22
The Influence of Specimen Size .....	22
The Influence of the Quenching Medium .....	24
SUMMARY .....	29
MODIFIED BARNACLE CELL .....	31
Materials and Procedure .....	31
RESULTS AND DISCUSSION .....	32
Rectangular, Bead-on-Plate, Weld Specimens ...	37
Spherical Decanted Weld Specimens .....	41
Steel-Shot Specimens .....	45
Sensitivity Analysis .....	62
Vacuum-Degassed Steel Shot .....	66
SUMMARY .....	68

THE RPI SILICONE-OIL EXTRACTION METHOD .....	71
Apparatus .....	71
Calibration .....	73
Materials and Procedure .....	75
RESULTS AND DISCUSSION .....	83
Determination of Diffusible-Hydrogen Content in HYL30 Weldments .....	84
Determination of Diffusible-Hydrogen Content in Soviet Steel 15Г2АφΔ (Steel 15) Weldments .....	86
Influence of Hydrogen Content on Extraction Time .....	93
Advantages of the RPI Silicone-Oil Extraction Method .....	98
SUMMARY .....	98
GENERAL CONCLUSIONS .....	101
Mass-Spectrometer Hot-Extraction Method .....	101
Modified Barnacle Cell Method .....	102
RPI Silicone Oil Extraction Method .....	103
REFERENCES .....	105

## LIST OF TABLES

	<u>Page</u>
Table 1	Chemical Composition of 14X2 MP Steel ..... 8
Table 2	Composition of As-Deposited AH -2 SMAW Electrodes ..... 9
Table 3	Summary of Welding Conditions ..... 10
Table 4	Diffusible Hydrogen Content of Weld Metal Specimens Using BWRA/IIW Method ..... 25
Table 5	Mass Spectrometer Analyses of Diffusible Hydrogen Content of Weld Metal Decant Specimens Quenched in Water ..... 26
Table 6	Mass Spectrometer Analyses of Diffusible Hydrogen Content of Weld Metal Decant Specimens Quenched in Liquid Nitrogen ..... 28
Table 7	Chemical Composition of Materials Used in the Modified Barnacle Cell Investigation ..... 33
Table 8	Preparation Conditions and Corrosion Potentials for Hydrogen-Charged, Blast-Cleaned, Steel-Shot Specimens ..... 46
Table 9	Preparation Conditions and Corrosion Potentials for Hydrogen-Charged, Steel- Shot Specimens Quenched Within a Non- Oxidizing Atmosphere ..... 48
Table 10	Diffusible Hydrogen Content of Steel- Shot Specimens ..... 49
Table 11	Calculated Extraction Currents ..... 51
Table 12	Comparison of Extraction Currents, $I_A$ , in Microamperes, From Lead Wires and From Shot Specimens With Lead Wires ..... 54
Table 13	Estimated Diffusible Hydrogen Content (ppm) and Diffusivity Values for Hydrogen- Charged, Grit-Blasted Specimens ..... 59
Table 14	Estimated Diffusible Hydrogen Content (ppm) for Hydrogen-Charged, Grit-Blasted Specimens ..... 61



Table 15	Estimated Diffusible Hydrogen Content (ppm) and Diffusivity Values for Hydrogen- Charged Specimens Quenched Within a Non-Oxidizing Atmosphere .....	63
Table 16	Estimated Diffusible Hydrogen Content (ppm) for Hydrogen-Charged Specimens Quenched Within a Non-Oxidizing Atmosphere .....	64
Table 17	Chemical Compositions of Material Used in the RPI Silicone-Oil Investigation .....	76
Table 18	Mechanical Properties of Material .....	77
Table 19	Summary of Welding Conditions .....	81
Table 20	Typical Data for a Low- and a High- Hydrogen Weld in HY-130 .....	85
Table 21	Typical Data for a Low- and a High- Hydrogen Weld in Steel 15 .....	94
Table 22	Data for a Low-Hydrogen Weld in Steel 15 ....	95

## LIST OF FIGURES

	<u>Page</u>
Figure 1      Schematic Views of the Decanting Procedure ..	11
Figure 2      Schematic Diagram of Gas Analyzer .....	13
Figure 3      Close-Up View of the Gas Analyzer .....	14
Figure 4      Monopole Partial Pressure Analyzer Electronics .....	15
Figure 5      Close-Up View of the Molybdenum Basket .....	16
Figure 6      Overall View of the Ion Gage and the Sample Holder .....	18
Figure 7      Overall View of the Mass-Spectrometer, Hot-Extraction Method .....	20
Figure 8      Instantaneous Hydrogen Evolution Data for a 500°C Extraction Temperature .....	23
Figure 9      Modified Barnacle Cell Apparatus .....	35
Figure 10     Schematic Diagram of Modified Barnacle Cell .	36
Figure 11     Extraction Transients from Rectangular Bead-on-Plate Specimens .....	39
Figure 12     Extraction Transients from Decant Weld Specimens .....	43
Figure 13     Computed Extraction Transients Utilizing Various Values of Diffusivity, D, for Spherical Specimens .....	52
Figure 14     The Effect of Lead Wires on Measured Extraction Transients .....	56
Figure 15     Extraction Transients from Run 1, Steel-Shot Specimens .....	57
Figure 16     Extraction from Charged, Uncharged, and Vacuum Degassed Steel-Shot Specimens .....	67
Figure 17     Diagram of RPI Silicone-Oil Apparatus .....	72
Figure 18     The RPI Silicone-Oil Apparatus .....	74

Figure 19	Schematic Illustration of the Welding Fixture and Specimen Arrangements .....	79
Figure 20	Semi-Automatic Stickfeeder Unit for Shielded Metal Arc Welding (SMAW) .....	80
Figure 21	Photomacrograph of a High-Hydrogen Weld Which Exhibits Porosity ( $\text{ppm}_d=18.6$ ) 5X .....	87
Figure 22	Correlation Between the RPI and BWRA/IIW Methods in $\text{ppm}_d$ of Diffusible Hydrogen in E-14018/HY-130 Weldments, Utilizing Deposited-Metal Weight, $\Delta W_d$ .....	88
Figure 23	Correlation Between the RPI and BWRA/IIW Methods in $\text{ppm}_c$ of Diffusible Hydrogen in E-14018/HY-130 Weldments, Utilizing Composite-Zone Weight, $W_c$ .....	89
Figure 24	Correlation Between the RPI and BWRA/IIW Methods in $\text{ppm}_d$ of Diffusible Hydrogen in Steel 15 Weldments, Utilizing Deposited-Metal Weight, $\Delta W_d$ .....	91
Figure 25	Correlation Between the RPI and BWRA/IIW Methods in $\text{ppm}_c$ of Diffusible Hydrogen in Steel 15 Weldments, Utilizing Composite-Zone Weight, $W_c$ .....	92
Figure 26	Sample 23 Which Exhibits a Negative $\Delta W_d$ , 5X .....	96
Figure 27	Plot of Extraction Volume of Diffusible Hydrogen ( $\Delta V$ ) vs. Time for a Low- and High-Hydrogen Weld .....	97

#### ACKNOWLEDGEMENTS

This program was supported by the Office of Naval Research, Metallurgy and Ceramics Program, under Contract No. N00014-75-C-0944. Technical monitoring of the program was provided by Dr. Bruce A. MacDonald. The authors greatly appreciate this financial and technical support.

The authors are indebted to Charles E. Arribehaute, Joris Naiman, William J. Gestal, Jr., and Doreen J. Ball, who participated in the research effort.

## ABSTRACT

Control of the hydrogen content in weldments is necessary to prevent hydrogen-induced cracking in high-yield-strength steels. Because a critical amount of diffusible hydrogen must be present for hydrogen-induced cracking, it is essential to determine the amount of hydrogen introduced by various welding procedures.

In this investigation, three methods for the determination of diffusible hydrogen content in weldments were developed and qualified: 1) a mass spectrometer hot-extraction method, 2) a modified Barnacle Cell electrochemical method, and 3) a silicone-oil extraction method.

In the mass-spectrometer hot-extraction method, a small sample of weld metal is heated in a high-vacuum system in which a mass spectrometer is used to analyze the partial pressure of the extracted hydrogen. If a suitable medium is discovered for quenching the weld-metal decant specimens, this method would provide a means for determining the diffusible and total hydrogen content of weld metals.

In the modified Barnacle Cell method, the diffusible hydrogen is electrochemically oxidized to water at the surface of the specimen. The resulting oxidation current, which is measured, is proportional to the hydrogen-evolution rate and should obey a diffusion law. This method could not be used satisfactorily to determine the diffusible hydrogen content of bead-on-plate weldments, because the

weld bead results in a non-rectangular geometry and a non-uniform hydrogen content. However, the Barnacle Cell method could be used to measure the diffusible hydrogen content of hydrogen-charged spherical specimens; unfortunately, the accuracy of the measurement is limited by the ability to estimate, accurately, the hydrogen diffusivity.

In the RPI silicone-oil extraction method, diffusible hydrogen in a sample is extracted at 100°C in hydrogen-saturated silicone oil and is collected in a burette. This method is a reliable, rapid, safe, and inexpensive technique for the determination of diffusible-hydrogen content in weldments. The use of the composite-zone weight, rather than the deposited weld metal weight, yielded a better consistency of results and a better correlation between these results and those obtained by the BWRA/IIW mercury extraction technique.

## INTRODUCTION

The development of high-yield-strength, structural steels has led to an increase in the problems associated with hydrogen-induced cracking (cold cracking). This cracking, which occurs in either the heat-affected zone or the weld metal, may appear immediately, or after prolonged periods of time, extending up to several weeks.

Four conditions are required, simultaneously, for hydrogen-induced cracking:

1. A critical concentration of diffusible hydrogen,
2. A critical level of local tensile stress,
3. A crack-susceptible microstructure, and
4. A sufficient amount of time in the crack susceptible temperature range (-100 to 200°C).

Critical stress levels and crack-susceptible microstructures are usually present in high-strength-steel weldments. Therefore, when the steels are used at ambient temperatures, control of the hydrogen content is mandatory to prevent hydrogen-induced cracking.

Hydrogen is introduced into weldments as a result of the dissociation of hydrogen gas, water vapor, and hydrogen-bearing compounds to produce atomic hydrogen in the welding arc. The major sources of hydrogen are moisture in the coating of SMAW electrodes, moisture and/or contaminants in GMAW shielding gas, contamination on the filler wire, and surface contaminants on the base metal.

Because a critical concentration of diffusible hydrogen must be present for hydrogen-induced cracking, it is essential to determine the amount of hydrogen introduced by various welding procedures. Several different techniques have been employed to determine the hydrogen concentration in steel weldments.

The British Welding Institute (BWRA), (Ref.1), developed a procedure for hydrogen determination in the 1960s which was subsequently adopted by the IIW. In the technique, a standard sample containing a weld deposit is stored in a vacuum over mercury at room temperature for 72 hours to extract the diffusible hydrogen. The hydrogen content is measured by volumetric methods and reported as ppm or as cc/100g of deposited weld metal. However, since the determination takes three days and no positive identification of the gas species evolved is possible, the system has definite limitations.

A carrier-gas technique developed at BWRA (Ref.2) involves heating a sample at 650°C (1202°F) in a stream of argon carrier gas and monitoring the change in thermal conductivity of the gas stream produced by the evolution of hydrogen from the sample. Boillot and Hanin (Ref.3) used the carburizing fusion technique in which the sample is melted in a nitrogen carrier gas. The variations of thermal conductivity of the carrier gas are integrated to determine the total hydrogen concentration. Although these techniques are efficient and rapid, the equipment required



is expensive.

A chromatographic method for the determination of diffusible hydrogen content was developed at the E. O. Paton Electric Welding Institute in the USSR (Ref.4). In this method, standard BWRA/IIW specimens are welded and placed in a reaction chamber which has been heated to 150°C. Argon, as a carrier gas, is passed through the chamber for 10 seconds carrying any evolved gases to a chromatograph which measures the amount of hydrogen. This procedure is repeated every 10 minutes for approximately 2 1/2 hours.

Diffusible hydrogen content has been analyzed by the electro-chemical determination of hydrogen concentration in metals utilizing the Barnacle-cell principle (Refs.5,9) This technique uses a Ni/NiO electrode with a NaOH solution as an electrolyte. The sample is made the anode, and the current required to convert the emerging atomic hydrogen to hydrogen ions is measured. A relationship between current density, diffusion coefficient, and initial hydrogen concentration can be derived for applicable boundary conditions with the aid of Fick's Laws. In previous work at RPI, difficulties have been noted in correlating the results of the Barnacle cell with those obtained by other methods for measuring the hydrogen content of welds.

The Japanese Glycerin Replacement Method (JIS), (Ref.10), involves the immersion of a suitable sample containing a weld deposit in a glycerin bath at 45°C and the collection of the hydrogen evolved in a buret. The test

procedure is simple, but the extraction requires approximately two days. This system also has serious shortcomings in that the results obtained are 35-40% lower than those obtained by the BWRA/IIW method and are inconsistent at low-hydrogen levels.

## OBJECT

This investigation involved the development and qualification of three methods for the determination of diffusible hydrogen content in weldments.

1. A hot-extraction method utilizing a mass spectrometer,
2. An electrochemical technique using a modification of the Barnacle Cell, and
3. A silicone-oil extraction method developed at RPI.

These methods will be discussed individually in the following sections.

## MASS-SPECTROMETER HOT-EXTRACTION METHOD

In this hot-extraction method, a small sample of weld metal is heated in a high-vacuum system. Hydrogen and other gases are extracted and passed through a calibrated orifice which is located between the measuring chamber and the vacuum system. A mass spectrometer analyzes the partial pressure of the evolved gases within the chamber and permits quantitative determination of the gas content in the sample.

### Specimen Preparation

Test specimens for the mass-spectrometer analysis were produced by decanting molten metal from the weld pool. Welds were deposited on a Soviet steel, 14x2ГMP, using a semi-automatic SMAW process with 4-mm (5/32-in) diameter matching electrodes, АНπ-2. The composition of the steel, the analysis of the deposited weld metal, and the welding parameters are presented in Tables 1, 2, and 3, respectively. In the decanting procedure, the base metal was clamped in a horizontal position on a hinged platen, as shown in Figure 1A. During welding, a spring-loaded weight was released and the platen rapidly accelerated downward. The molten weld was decanted in this fashion and collected in a basin containing a quenching medium, as illustrated schematically in Figure 1B. In this manner, nearly spherical samples of weld metal were collected which ranged from 2 to 4-mm (0.078 to 0.016-in) in diameter. These decanted specimens

TABLE 1

Chemical Composition of 14X2TMP Steel\*

C	0.18%	Ni	0.07%
Mn	1.09	Mo	0.52
Si	0.27	S	0.019
V	0.03	P	0.013
Cr	1.62	B	0.002-0.006

\*USSR Quench-and-Tempered Steel with 85,000 psi ( $60 \text{ kg/mm}^2$ )  
Yield Strength.

TABLE 2

Composition of As-Deposited  
AH $\pi$ -2\* SMAW Electrodes

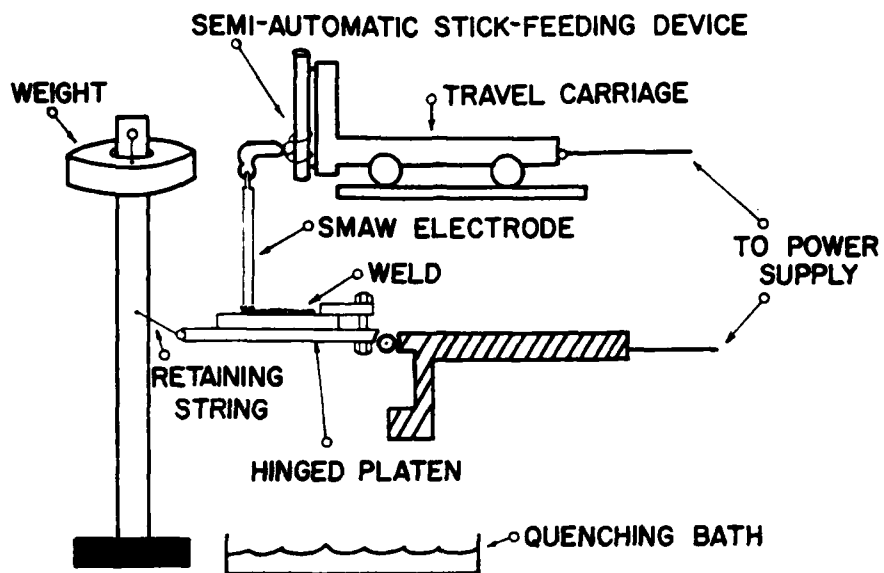
C	0.062%	Ni	2.08%
Mn	0.95	Cr	0.99
P	0.017	Mo	0.37
S	0.015	V	0.040
Si	0.21		

\*USSR SMAW Electrodes roughly equivalent to E-10018.

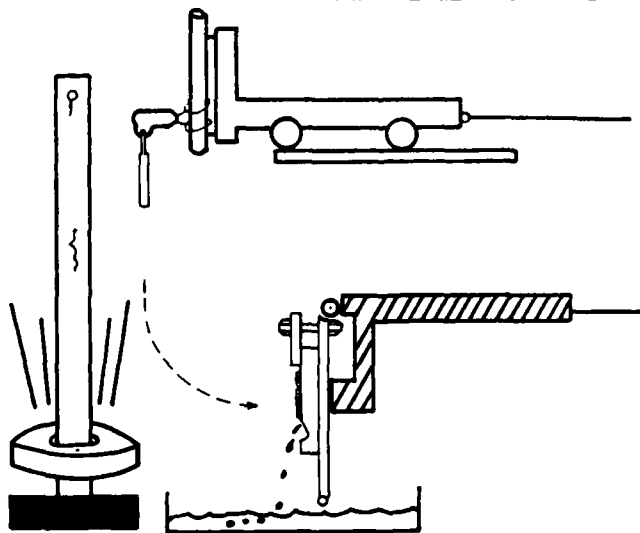
TABLE 3

Summary of Welding Conditions

Arc voltage	20 V
Current	170 Amps
Travel speed	5 ipm (12.7 cm/min)
Preheat temperature	150°C (302°F)
Electrode preparation	
High H <sub>2</sub> practice	electrodes contaminated by soaking in water
Low H <sub>2</sub> practice	Heated to 420°C (788°F), held for 1 hour, furnace cooled to 150°C (302°F) and stored at this temperature.



**A. WELDING OPERATION**



**B. QUENCHING OPERATION**

**Figure 1. Schematic Views of the Decanting Procedure.**



were temporarily stored in a dry ice-alcohol mixture at  $-70^{\circ}\text{C}$  ( $-94^{\circ}\text{F}$ ) and subsequently transferred to liquid nitrogen,  $-196^{\circ}\text{C}$  ( $-320^{\circ}\text{F}$ ), minimize loss of diffusible hydrogen.

As a basis for comparison, welds were made using the low-hydrogen practice recommended for these Soviet-produced materials and the hydrogen content was determined by the BWRA/IIW method. The results indicated that the conditions listed in Table 3 gave diffusible hydrogen levels of approximately 5-ppm (5.5cc/100g) of deposited weld metal.

### Apparatus

Figure 2 is a schematic diagram of the gas analyzer. The gas analyzer uses a monopole-type mass spectrometer, (Ref.11) visible as the inclined cylindrical appendice at the right in Figure 3.

A schematic diagram of the monopole-type partial pressure analyzer is shown in Figure 4. The signal delivered by the detector is amplified by an electrometer amplifier and routed to a strip-chart recorder and a cathode-ray oscilloscope. This type of mass spectrometer has been reported to be capable of measuring partial pressures as low as  $10^{-14}$  torr with a mass range from 1 to 300.

The extraction chamber is equipped with a glass window and contains a resistance-heated basket, which is visible in Figure 5, in the form of a conical-coil wound from 1-mm

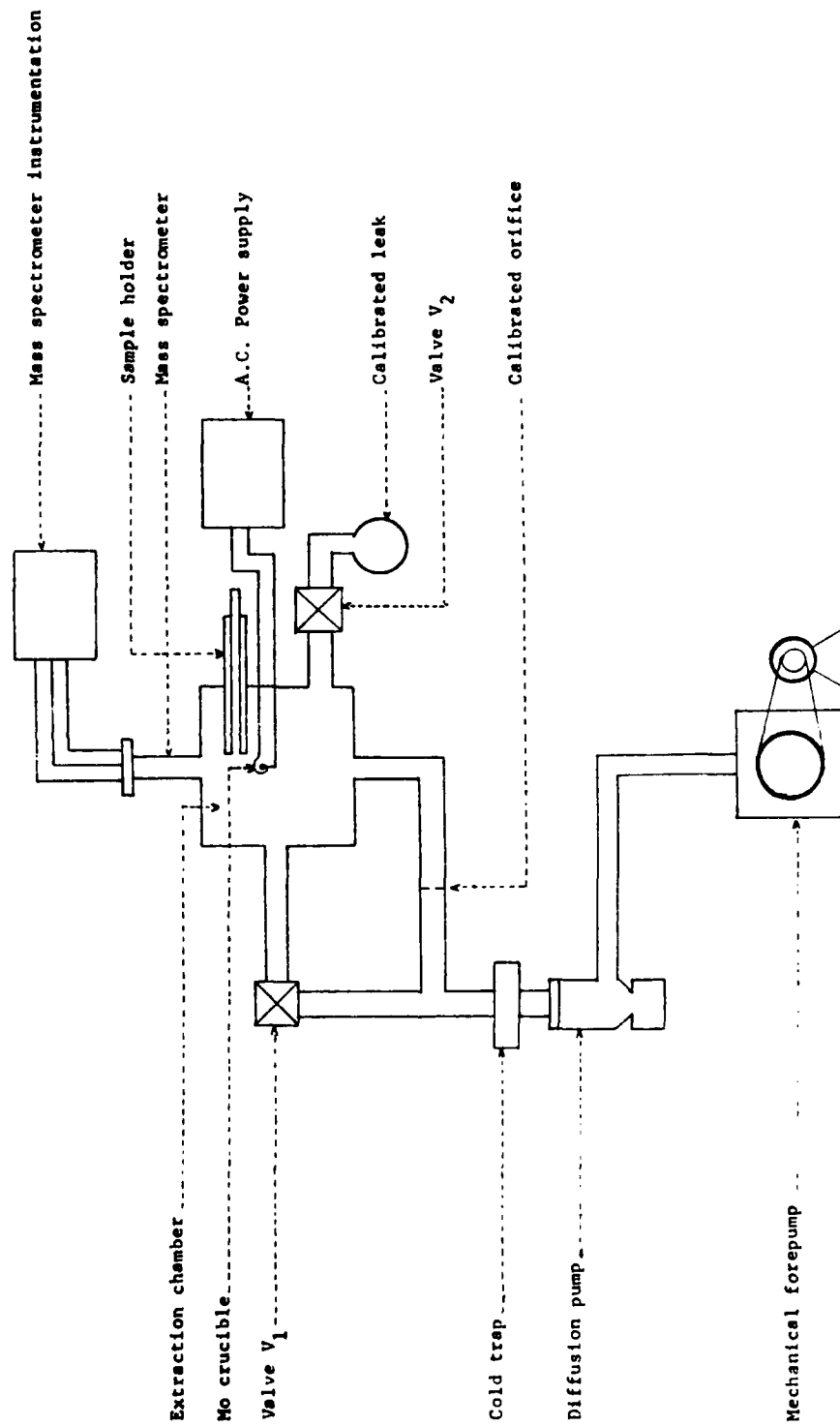


Figure 2. Schematic Diagram of Gas Analyzer.

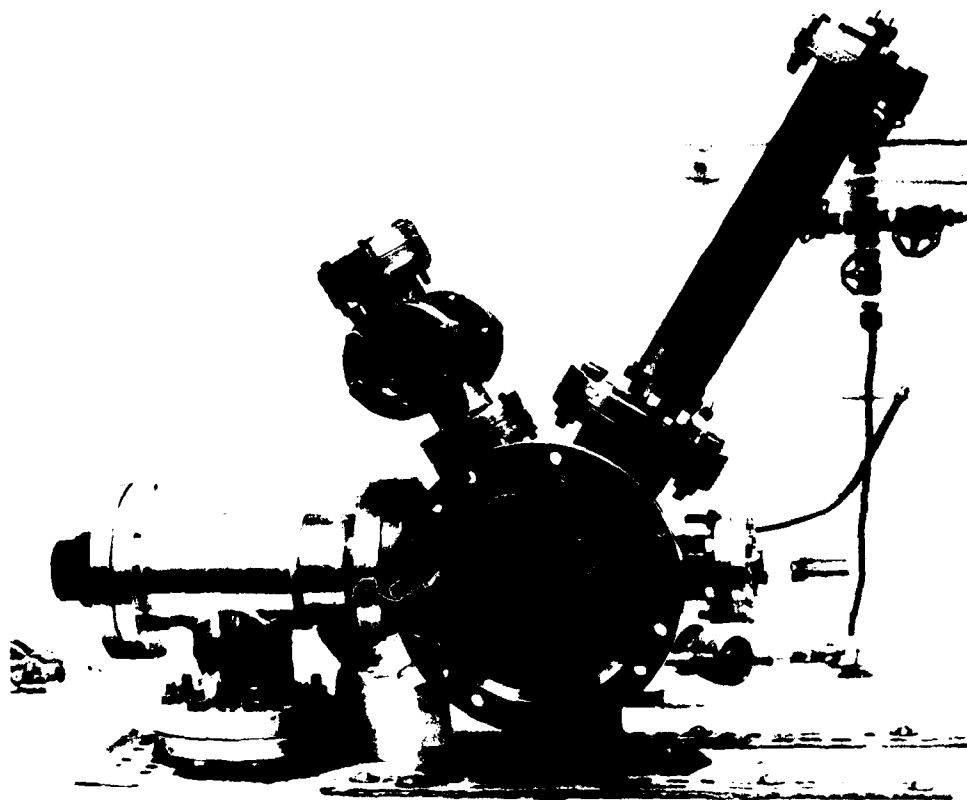


Figure 3. Close-Up View of the Gas Analyzer.

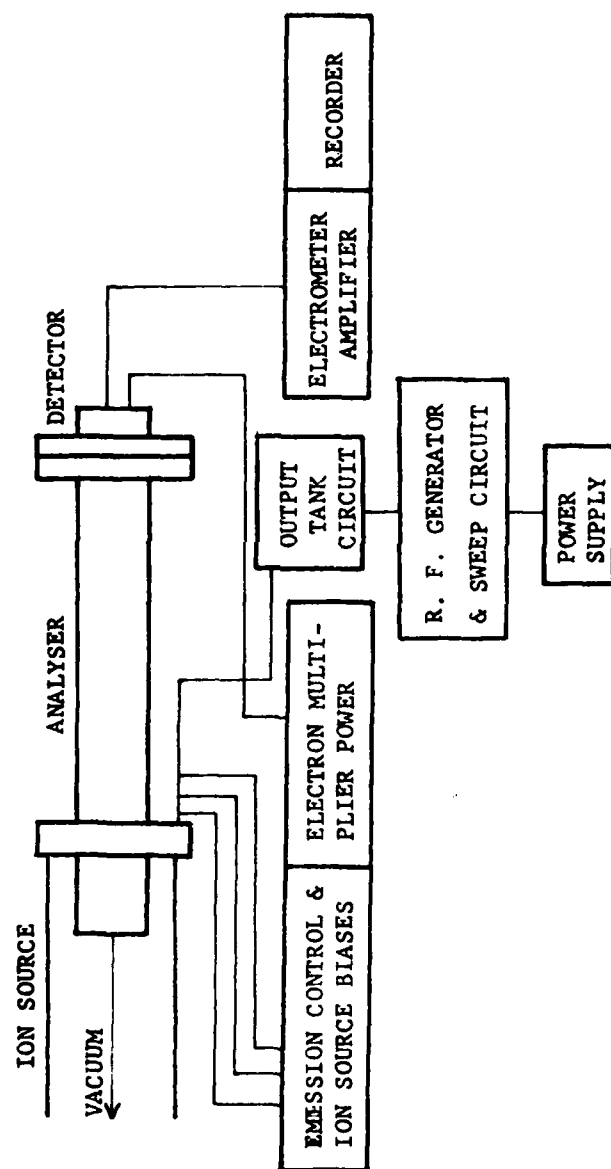


Figure 4. Monopole Partial Pressure Analyzer Electronics.

Figure 5. Close-Up View of the Molybdenum Basket.



(0.040-in) diameter molybdenum wire. Current from the AC power supply, shown at the right in Figure 2, is adjusted to heat the molybdenum basket to the extraction temperature of 500°C (932°F). Molybdenum was used for the basket material because there is little interaction with the steel samples and, after the completion of the analysis at 500°C, the temperature of the basket could be raised to melt the sample and obtain total hydrogen content.

The retractable sample holder, visible in the center of Figure 5 just above the heating basket, is located on a rod contained within an evacuated side chamber. The holder is manipulated by an external magnet (visible at lower left in Figure 6) to introduce the specimens to the extraction chamber and transfer them one at a time to the molybdenum basket. The specimen holder and the specimens were cooled with liquid nitrogen until transfer to the molybdenum basket to prevent premature loss of hydrogen.

The main vacuum valve,  $V_1$ , was positioned between the extraction chamber and the vacuum system. A cold trap was located just above the diffusion pump, as shown in Figure 2, to prevent contamination of the chamber by oil vapor from the diffusion pumps.

To facilitate calibration of the gas analyzer, a 3.09-mm diameter, calibrated orifice by-passed the main vacuum valve,  $V_1$ , and a calibrated leak (flow of hydrogen) entered the extraction chamber through valve  $V_2$ , as indicated in Figure 2. Valve  $V_2$  is visible just below the right rear of

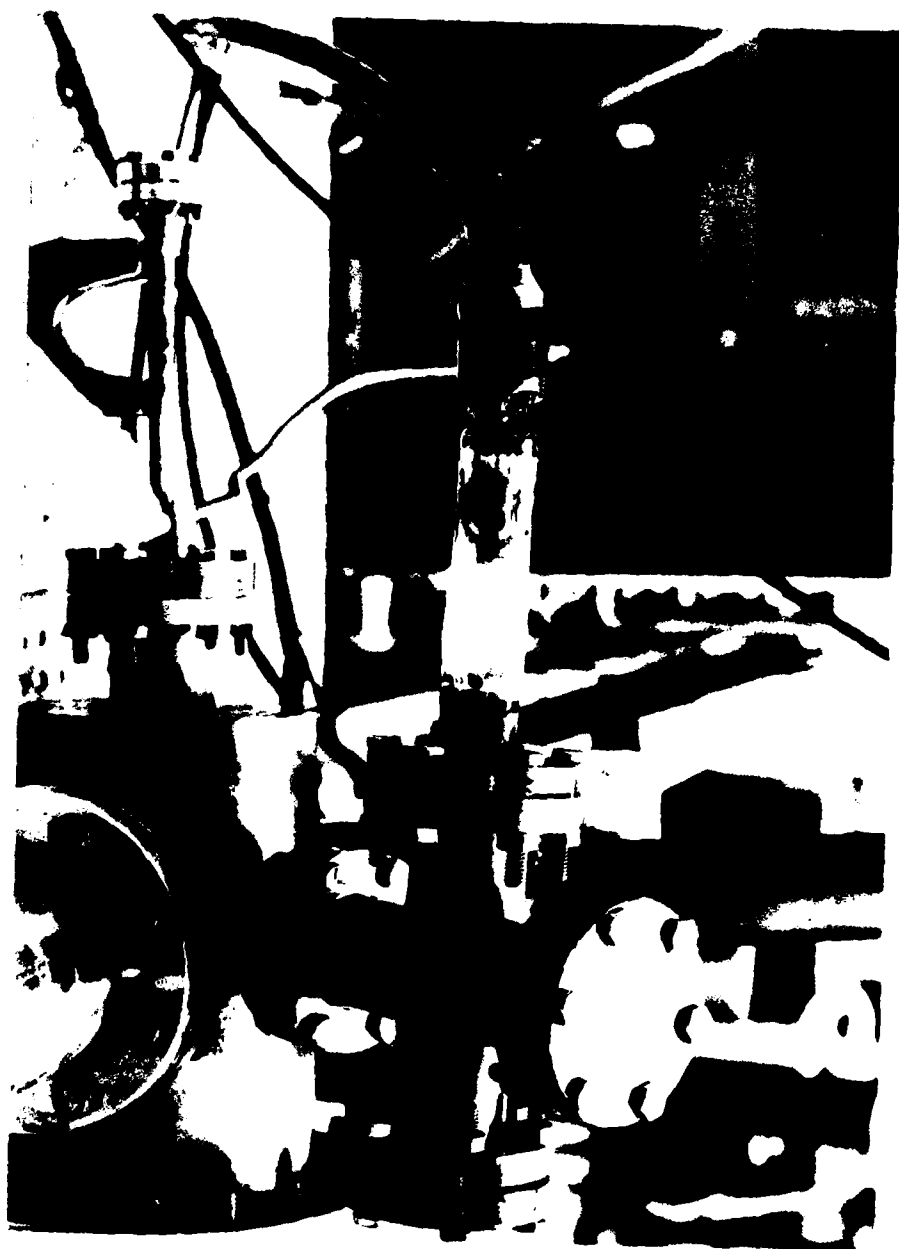


Figure 6. Overall View of the Ion Gage and the Sample Holder.

the extraction chamber in Figure 3.

Figure 7 is an overall view of the apparatus with the auxiliary electronics and recording equipment rack-mounted at the right.

#### Calibration of Apparatus

After pumping the chamber of  $10^{-5}$  torr, the mass spectrometer was tuned to the  $M/e = 2$  peak arising from  $H_2$  in the gas phase contained within the extraction chamber. The mass-spectrometer signal was calibrated with a flow of hydrogen into the chamber from a calibrated leak source at a rate of  $6.84 \times 10^{-6}$  cc/sec  $\pm 1\%$  (converted to STP). During calibration the main vacuum valve,  $V_1$ , was closed so that the 3.09-mm diameter, calibrated orifice provided the only means of escape to the vacuum system.

When the partial pressure of hydrogen reached a value such that the rate of escape through the calibrated orifice just equalled the rate of entry through the calibrated leak, a condition of dynamic equilibrium was achieved as follows:

From the manufacturer's calibration value,  $Q_L = 6.84 \times 10^{-6}$  STP cc/sec.

According to the kinetic theory,

$$Q_L = P_L \times S$$

where:  $P_L$  = reference partial pressure of  $H_2$  (in torr) from the calibrated leak.

$S$  = conductance (in liters/sec) of the calibrated orifice.



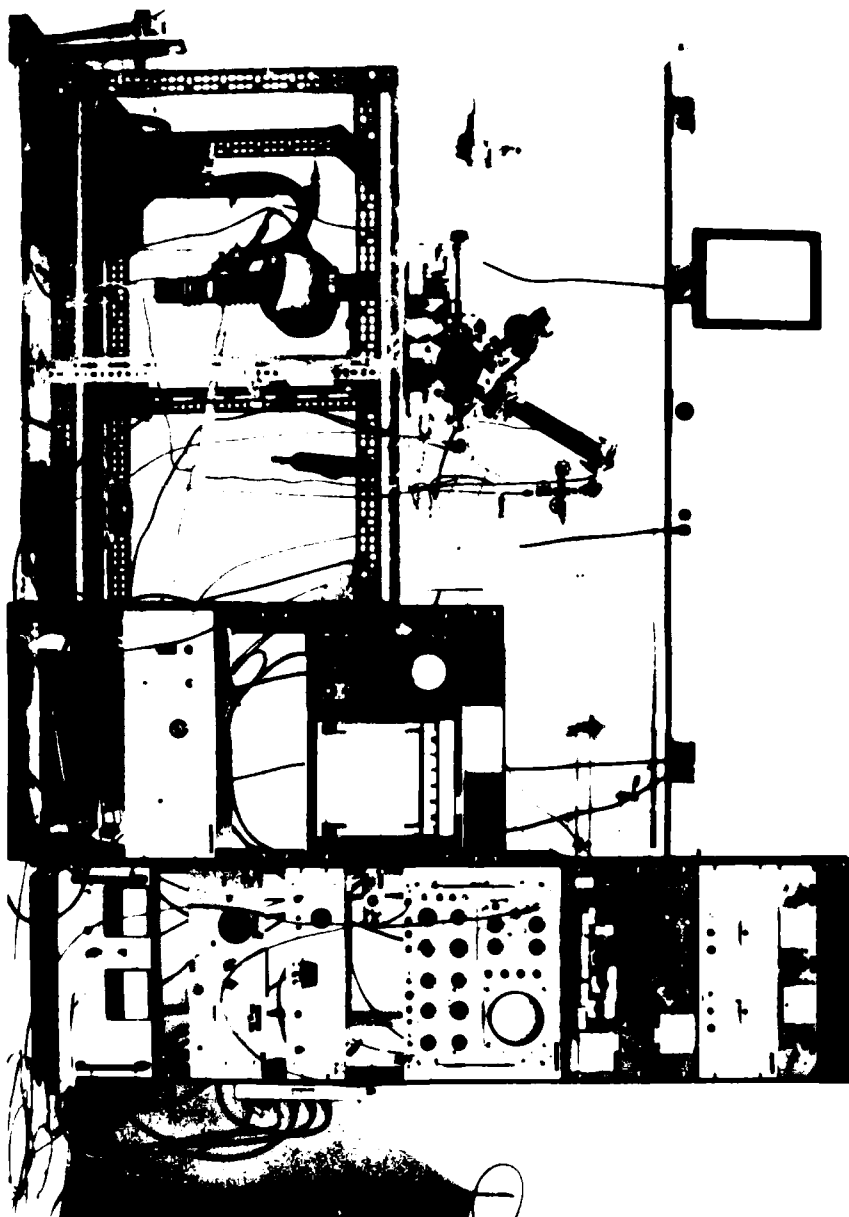


Figure 7. Overall View of the Mass-Spectrometer Hot-Extraction Method.

For the capillary opening through which the gas escapes from the extraction chamber, S may be calculated from:

$$S = 11.6 \times A \times \frac{M_{H_2}}{M_{air}}^{1/2}$$

where: A = area in  $cm^2$

$M_{air}$  = molecular weight of air (in grams)

$M_{H_2}$  = molecular weight of hydrogen (in grams)

For the 3.09-mm diameter orifice used in this investigation, a value  $S = 230$  cc/sec is obtained.

The mass spectrometer current  $I_{ms}$  recorded is proportional to  $P_L$ , so that,

$$P_L = k I_{ms}$$

where k is a constant

Therefore:  $Q_L = k I_{ms} S$

With the main valve,  $V_1$ , and the calibrated leak valve,  $V_2$  closed, a record of background pressure in the chamber is obtained. The calibrated leak valve,  $V_2$ , is then opened and the system pressure allowed to achieve dynamic equilibrium with the main valve,  $V_1$ , closed. The difference in mass spectrometer output between these two conditions correspond to the term  $I_{ms}$  in Equation 4 and allows evaluation of the constant k.

#### Analytical Procedure

Specimens were weighed and placed in the sample holder which was already at liquid-nitrogen temperature,  $-196^\circ C$

(-320°F). Before the actual analysis, pressure in the extraction chamber was reduced to approximately  $10^{-5}$  torr and the molybdenum basket was heated and maintained for at least two minutes at about 1400°C (2552°F) for outgassing. After outgassing, the temperature of the molybdenum basket was reduced to 500°C (932°F), the actual analysis temperature. Valve  $V_1$  was closed and, as a result, the extraction chamber was evacuated through the 3.09-mm diameter calibrated orifice. To extract hydrogen, the sample was then placed in the preheated molybdenum basket.

During the extraction, the hydrogen partial pressure was measured on the previously calibrated, strip-chart recorder. The hydrogen content was determined by integration of the hydrogen partial pressure as a function of time, as recorded by the strip-chart-recorder.

Because concentration values were referred to as cc of hydrogen per 100 grams of added filler metal, or as ppm (1 ppm = 1.1 cc/100g), it is necessary to evaluate the dilution rate in the welds. Metallographic determination of etched welds showed that 5-cm (2-in) long weld beads had a dilution rate of approximately 45%, i.e., 45% of the total weld metal was base metal.

## RESULTS AND DISCUSSION

### The Influence of Specimen Size

Figure 8 shows data for instantaneous hydrogen evolution as a function of time obtained from two different samples

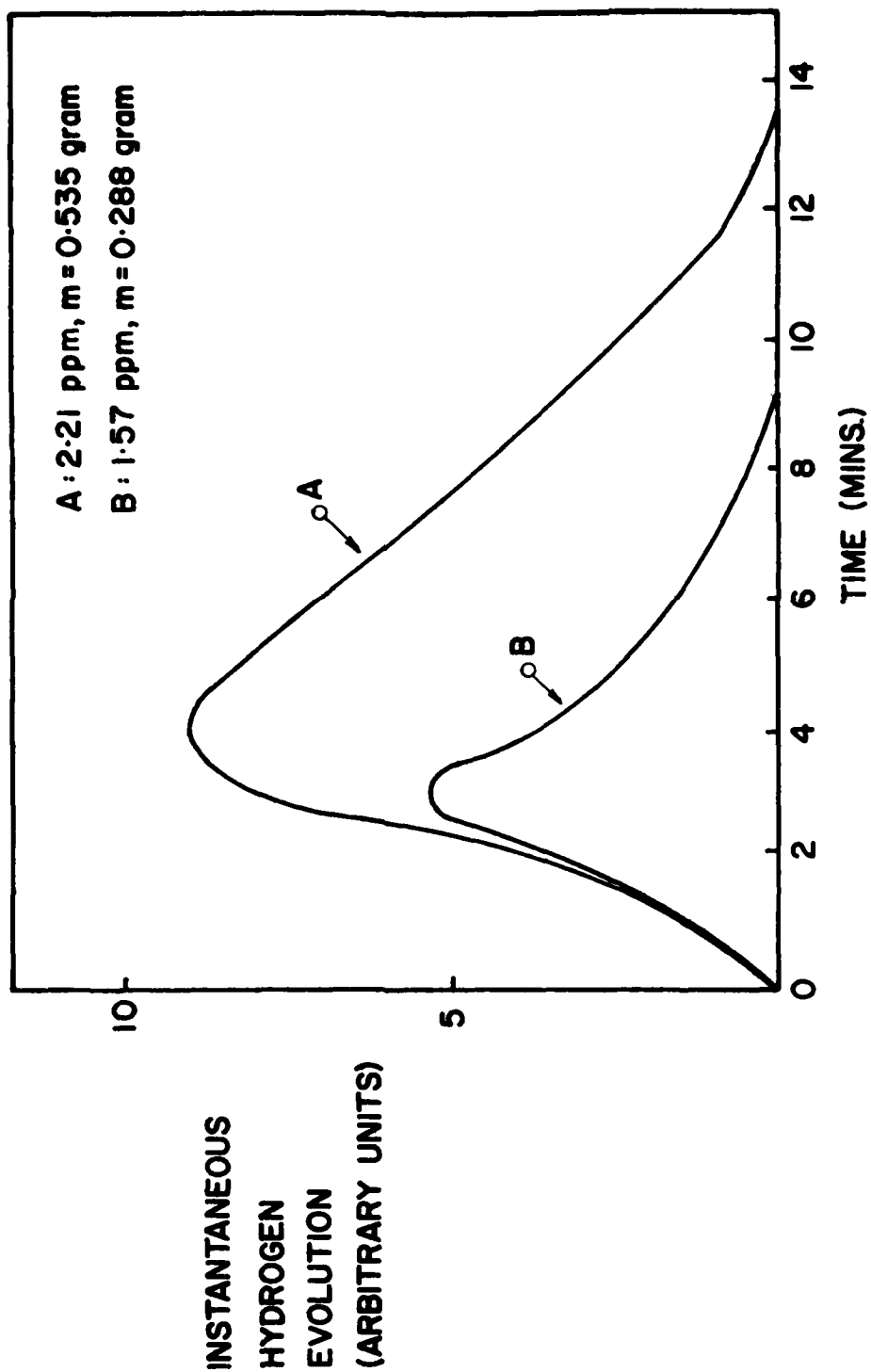


Figure 8. Instantaneous Hydrogen Evolution Data for a 500°C Extraction Temperature.

which contained approximately the same hydrogen content, 1.9 ppm. With a sample weighing 0.535 gram, the total amount of gas was extracted at 500°C (932°F) in about 13 minutes, whereas with a sample weighing 0.288 gram, only 9 minutes were necessary to extract the hydrogen. Thus, the rate of extraction and the time required for extraction varied with the size of the specimen.

#### The Influence of the Quenching Medium

The hydrogen contents of the decanted specimens, determined by the standard BWRA/IIW technique, are presented in Table 4. The mean value, 5.10 ppm, was taken as a reference to compare with the data obtained in this investigation.

Test specimens for the mass spectrometer were produced utilizing water as a quenching medium. Droplets of the liquid weld metal fell into a basin filled with water and, subsequently, were transferred to a dry ice and alcohol bath -70°C (194°F). Water was chosen as the initial quenching medium because it has a higher heat capacity and is a more efficient quenchant than a dry ice-alcohol mixture.

Table 5 lists results obtained with the mass spectrometer when water was used as a quenching medium. The hydrogen content of the decant specimens determined by using the mass spectrometer was more than three times the value which was obtained utilizing the BWRA/IIW procedure.

This result is in agreement with that of Japanese

TABLE 4

Diffusible Hydrogen Content of Weld Metal  
Specimens Using BWRA/IIW Method

<u>Specimen Number</u>	<u>Hydrogen Content (ppm)</u>
05	4.9
07	5.2
010	4.8
011	5.8
Mean	5.2

TABLE 5

Mass Spectrometer Analyses of  
Diffusible Hydrogen Content of Weld Metal  
Decant Specimens Quenched in Water

<u>Diffusible Hydrogen Content (ppm)</u>			
<u>Weld Run</u>	<u>Sample Weight(g)</u>	<u>Individual</u>	<u>Weld Run Mean</u>
1	0.179	17.5	18.9
	0.070	17.3	
	0.059	21.9	
2	0.211	18.5	18.2
	0.079	17.3	
	0.056	18.8	
3	0.454	15.4	16.8
	0.043	15.2	
	0.380	19.9	
4	0.100	16.6	17.1
	0.165	17.5	
Overall Mean - 17.8			

investigators who found that the average hydrogen level of decanted specimens was approximately four times that of welds allowed to solidify naturally (Ref.10). It was not reported whether the high hydrogen levels in the decants were a result of quenchant dissociation, retention of weld pool hydrogen, cracks or porosity.

It was thus suspected that when the liquid weld metal was falling into the water, it was dissociating the surrounding water into atomic hydrogen. This hydrogen diffused into the lattice of the solidifying weld metal and led to the high results observed. To varify this assumption, a decant was made using a hydrogen-free quenching medium. With carbon tetrachloride ( $\text{CCl}_4$ ) as the quenching medium, the amount of diffusible hydrogen was in the range of 2.5 ppm, as shown in Table 6. This demonstrates that water could no longer be used as a quenching medium unless the flight path of the droplets was increased to allow solidification to be complete before entering the quenching bath. Also, the hydrogen level was lower than the reference value, because  $\text{CCl}_4$  is a less efficient quencher.

Table 6 summarizes the influence of a liquid nitrogen quenching medium on hydrogen content. The mean value was 2.56 ppm, approximately half than the reference value. Liquid nitrogen is poor quencher. Even though liquid nitrogen is at a very low temperature ( $-196^\circ\text{C}/-320^\circ\text{F}$ ), a vapor blanket forms during the quench and slows cooling of the specimens. An attempt was made to decant the weld pool



TABLE 6

Mass Spectrometer Analyses of  
Diffusible Hydrogen Content of Weld Metal  
Decant Specimens Quenched in Liquid Nitrogen

<u>Weld Run</u>	<u>Sample Weight(g)</u>	<u>Diffusible Hydrogen Content (ppm)</u>	
		<u>Individual</u>	<u>Weld Run Mean</u>
5	0.577	3.1	2.9
	0.090	2.7	
6	0.222	3.1	3.5
	0.223	3.8	
7	0.118	2.4	2.5
	0.260	2.9	
	0.120	2.3	
	0.121	2.2	
	0.101	1.9	
8	0.288	1.6	1.9
	0.535	2.2	
	0.105	2.4	
9	0.088	2.5	2.4
	0.314	2.8	
	0.818	1.8	
10	0.125	2.5	2.2
	0.472	2.0	
Overall Mean			2.6

utilizing splat cooling, but it was impossible to obtain spherical specimens.

Producing specimens proves to be difficult because of the quenching problem. Hence, it is necessary to find a hydrogen-free quenching medium which could slow down hydrogen diffusion out of the sample. This could be achieved by using a fluorocarbon refrigerant such as  $C_2Cl_4F_2$  (boiling point:  $92.8^{\circ}C$  ( $199^{\circ}F$ )). An alternate method that perhaps offers greater promise is to increase the length of the flight path of the decanted droplets to permit them to solidify before entering the quenching medium.

#### SUMMARY

A decanting method has been devised to produce weld metal samples for hot-extraction analyses of hydrogen. However, water, carbon tetrachloride, and liquid nitrogen were not suitable quenchants for the decanted weld-metal specimens. Utilizing the mass spectrometer, the hydrogen content of samples quenched in water was three times the expected value. The molten weld-metal decant dissociates the surrounding water which produces atomic hydrogen. This hydrogen is absorbed, readily, by molten decant and, thus, increased the total hydrogen content of the specimen. Decant specimens, quenched in liquid nitrogen and carbon tetrachloride, contained hydrogen which was approximately one

half the expected value. These quenching media produced a slow rate of cooling which enabled hydrogen to diffuse from the specimens.

If a suitable quenching medium is discovered, the mass spectrometer hot-extraction method would provide a means for determining the hydrogen content of decanted weld-metal samples.

## MODIFIED BARNACLE CELL

The Barnacle Cell was developed as a tool for determining the diffusible hydrogen content,  $C_0$ , of a steel specimen. (Refs.5-9) In this electrochemical method, a nickel/nickel oxide cathode maintains zero hydrogen content at the surface of the steel anode by oxidation of the evolved hydrogen to form water. The resulting oxidation current, which is proportional to the hydrogen-evolution rate, varies as a function of time. Because the steel is passive in the alkaline electrolyte, background currents, which might result from corrosion actions, have been reported to be relatively low. The evolution of hydrogen from a sample should obey a diffusion law. Thus, to determine  $C_0$  within a practical time-frame, the total oxidation current transient need be sampled only for a short interval. To convert this current-transient sample to a full transient, and a  $C_0$  value, the current-transient must be matched to a diffusion solution.

The original configuration of the Barnacle Cell was modified to enable the replacement of the Ni/NiO electrode with a potentiostat. In addition, the cell was modified to permit complete submersion of the samples in the 0.2N NaOH electrolyte.

### Materials and Procedure

Specimens of various compositions and shapes were used

in the modified Barnacle Cell investigation. Initially, tests were conducted with rectangular specimens, 7.5 x 12 x 18 mm, which were prepared according to BWRA/IIW test procedure. (Ref.1) The specimens, prepared from a low-alloy, quenched-and-tempered Soviet steel, 14X2ГMP, were welded using a semiautomatic SMAW process. The composition of this steel was presented previously in Table 1. The composition of the as-deposited weld metal derived from the 4-mm, E-7018 electrodes used in the SMAW process is given in Table 7.

Subsequently, tests were performed on spherical specimens produced by decanting molten weld-pool metal into a quenching medium. Using water-contaminated E-14018 coated electrodes, these decant specimens were produced from weldments on HY-130 base metal as previously described in the section: Mass Spectrometer, Materials and Procedure. The compositions of the HY-130 steel and the as-deposited E-14018 weld metal are shown in Table 7.

The final tests were conducted using 0.324-cm (0.128-in) diameter AISI 1008 steel shot. The hydrogen content of the shot was increased to approximately 2.0 ppm ( $1 \text{ ppm} = 1 \times 10^{-4} \%$  by weight) by heat treatment at 955°C (1751°F) in hydrogen at one atmosphere pressure. After charging, the first group of specimens were quenched into a dry ice-alcohol bath and were cleaned by grit blasting. The final group of steel shot was transferred from the charging furnace to the dry ice-alcohol quenchant in an inert atmosphere to prevent surface

TABLE 7

Chemical Composition of Materials  
Used in the Modified Barnacle  
Cell Investigation

<u>Material</u>	<u>C</u>	<u>Mn</u>	<u>P</u>	<u>S</u>	<u>Si</u>	<u>Ni</u>	<u>Cr</u>	<u>Mo</u>	<u>V</u>
HY-130	0.11	0.88	0.003	0.003	0.35	4.95	0.53	0.50	0.08
E-7018*	0.07	0.90	0.011	0.015	0.50	-	-	-	-
E-14018*	0.066	0.96	0.004	0.004	0.37	3.53	0.46	0.78	0.01

\*As-Deposited Analysis

oxidation and to obviate the necessity for grit blasting. Hydrogen-free control specimens were produced by vacuum degassing the steel shot at 1050°C.

All specimens were percussion welded to low-carbon-steel lead wires of 0.041-cm (0.016-in) diameter to provide an electrical connection.

The modified Barnacle Cell, shown in Figure 9, was constructed and prepared in accordance with standard electrochemical practice. (Ref.12) Figure 10 is a schematic diagram of the apparatus. Essentially, the modified cell is the extraction side of the Devanathan and Stachurski permeation apparatus. (Ref.13) Instead of a large plate specimen, a small specimen, a, is completely immersed in one liter of 0.2N NaOH electrolyte, c. The driving electrode is replaced by a potentiostatic power supply, e, operating from a voltage regulator, q. Oxidation current is read with a milliammeter, r, and anodic potential is determined with a sensitive electrometer, s, which has an output impedance of  $10^{10}$  ohms.

It should be noted in Figure 10 that two separate circuits are connected to the cell. The saturated-calomel reference electrode, i, is electrically connected to the specimen by ionic conduction. The ionic current path is through the saturated potassium chloride solution, t, the sodium hydroxide solution in the salt bridge, u, and the Luggin capillary, v. Thus, the calomel potential of the anodic specimen can be monitored via the circuit a-s-i-t-u-v-a. The connections at the potentiostat are tie points,

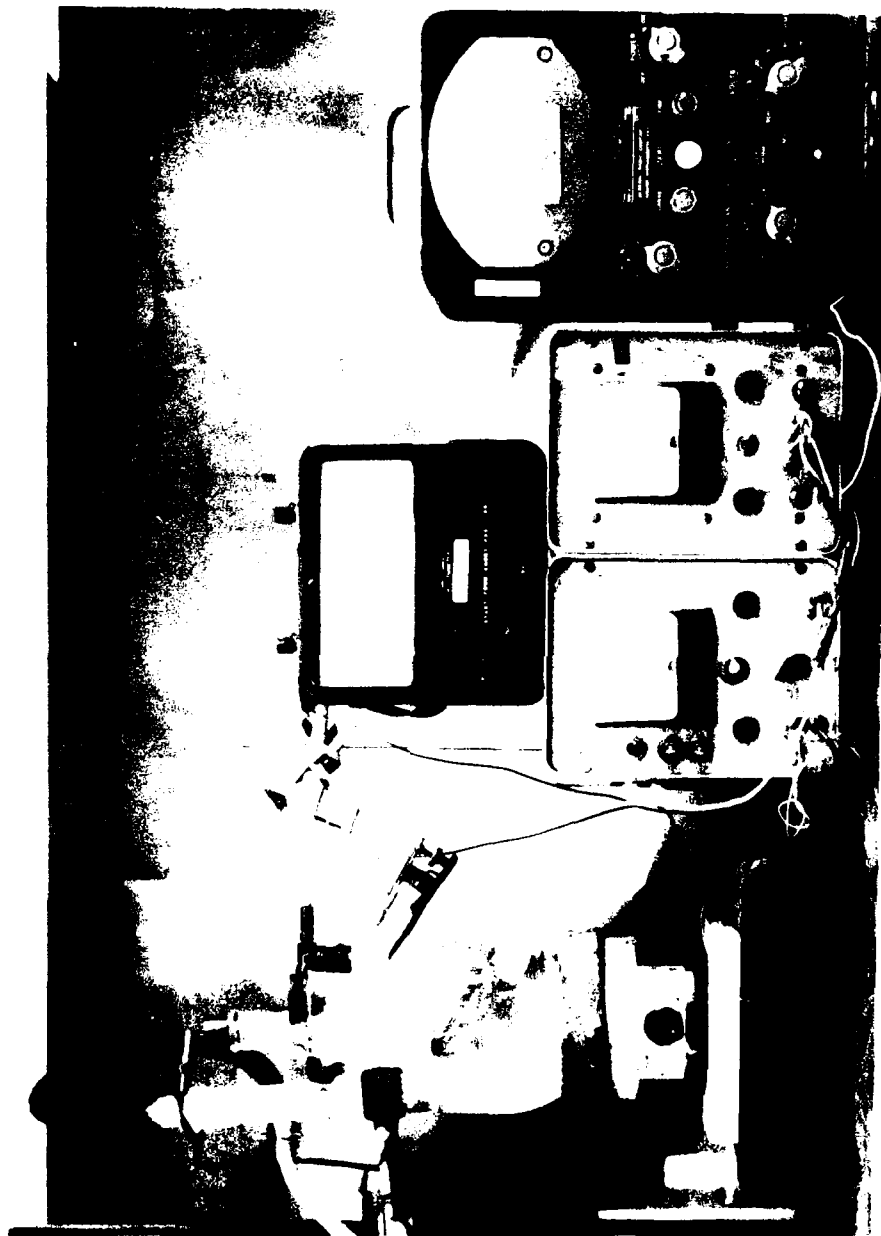
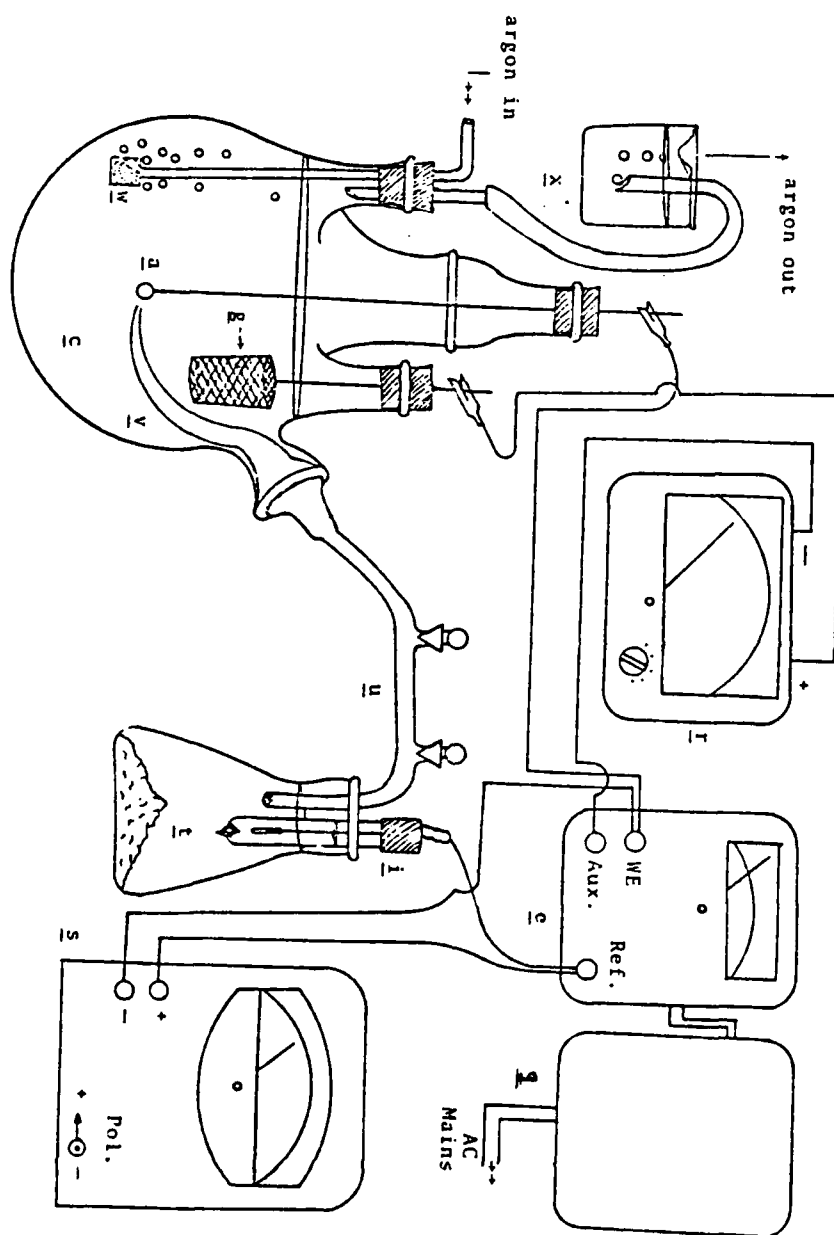


Figure 9. Modified Barnacle Cell Apparatus.



Figure 10. Schematic Diagram of Modified Barnacle Cell.



but the working electrode terminal (WE) is isolated from the reference electrode terminal (REF). The potentiostat output voltage is applied between WE and the auxiliary electrode (AUX) terminal. The oxidation current is supplied to the platinum-basket electrode, g, via the circuit a-g-r<sup>+</sup>-r<sup>-</sup>(AUX)-(WE)-a. This path is written in the direction of positive current flow.

### RESULTS AND DISCUSSION

Specimens were produced under various conditions and tested for hydrogen content in the modified Barnacle Cell. Transients of the extraction current as a function of time were recorded for comparison with transients predicted by solutions to diffusion equations. Specimens included three types: 1) rectangular, bead-on-plate, weld samples; 2) spherical weld-metal decants; and 3) steel shot which were prepared either by furnace charging in a hydrogen atmosphere or by vacuum degassing. Transient data, current as a function of time, are plotted in logarithmic coordinates to facilitate comparison with theoretically predicted curves.

#### Rectangular, Bead-on-Plate, Weld Specimens

Two rectangular weld specimens, which were prepared using the BWRA/IIW procedure, and one unwelded, rectangular, control specimen were tested. Initial corrosion potentials averaged -940 mv, saturated calomel electrode (S.C.E.)

for the welded specimens, and -700 mv for the control specimen. The extraction transients are shown in Figure 11. The curves labelled 1, 2, and 3 are the extraction current-time transients for the control and for the two welded specimens, respectively.

Gileadi<sup>(Ref.14)</sup> has proposed the following solution to the diffusion equation for planar conditions:

$$\frac{J^+}{zF} = C_0 \left(\frac{D}{\pi t}\right)^{1/2} \left[ 1 - \sum_{n=0}^{\infty} \left( -1^n \exp\left(-\frac{(n+1)^2 L^2}{Dt}\right) \right) \right]$$

where  $J^+$  is the current density in amperes/cm<sup>2</sup>,  $z$  is the valence of the dissolved hydrogen, which is equal to unity when  $C_0$ , the initial hydrogen concentration, is given in moles/cm<sup>3</sup>,  $D$  is the diffusivity in cm<sup>2</sup>/sec,  $F$  is Faraday's constant (96,487 coulombs/equivalent weight in grams),  $L$  is the diffusion distance in cm, and  $t$  is the time in seconds.

This solution can be approximated by one term for times  $t < L^2/4D$ . Assuming that  $L$  is 1/2 of the 0.75-cm specimen thickness and selecting  $D$ , conservatively, at  $10^{-6}$  cm<sup>2</sup>/sec at 20°C, there is ample margin for use of the approximate solution for times less than 10 hours. Under these conditions, Gileadi's solution simplifies to:

$$I_A = A F z C_0 (D/\pi)^{1/2}$$

where  $I_A$  is the extraction current in amperes and  $A$  is the anodic area in cm<sup>2</sup>.

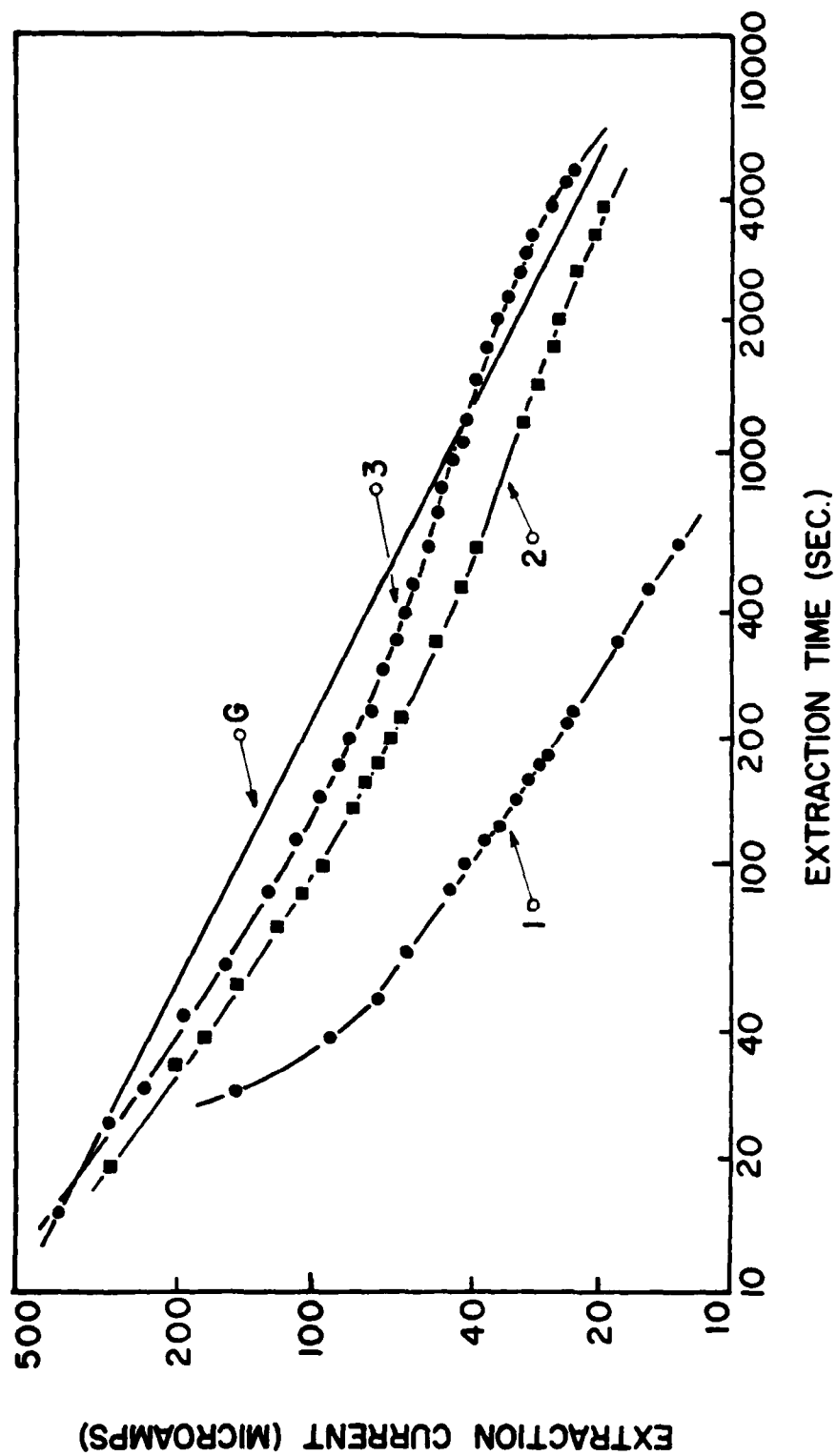


Figure 11. Extraction Transients from Rectangular Bead-on-Plate Specimens.

Inspection of the above approximation shows that the  $\log I_A$  is equal to  $-1/2 \log t$  plus the constant,  $\log(A F z C_0 \sqrt{D/\pi})$ . Thus, a plot of the equation on logarithmic coordinates yields a straight line with a slope of  $-1/2$  and an intercept equal to the constant. It should be noted that a variation in the anodic area, initial hydrogen concentration, or diffusivity is predicted to change only the vertical position of the line, and not its slope.

A graph of the equation,  $\log I_A = k - 1/2 \log t$ , is shown as Line G in Figure 11. The value of the constant,  $k$ , has been adjusted such that the computed transient, G, coincides with the observed current from Specimen 3 at  $t=15$  seconds. It should be noted that the observed transients are parallel to Line G for only short periods of time. The lack of agreement between the computed transient and the observed ones suggests that Gileadi's planar-diffusion model is not an accurate representation of the extraction of hydrogen from the rectangular specimens in the modified Barnacle Cell.

Computations made at different extraction times result in different estimated  $C_0$  values. For example, in Figure 11 at  $t=300$  seconds and 1000 seconds, the estimated  $C_0$  values for Specimen 3 are 2.8 and 2.0 ppm, respectively. This shift of  $C_0$  values with time also implies that the application of the Gileadi planar diffusion model to the welded rectangular specimens is inappropriate.

Two problems arise when the planar-diffusion model is applied to the extraction of hydrogen from BWRA/IIW specimens:

1) the non-planar geometry of the weld bead, and 2) the non-uniform hydrogen concentration. The addition of the weld-bead, which may be represented by an irregular semi-cylinder, changes the surface geometry of the specimen and increases the anodic area. Because hydrogen migrates to the heat-affected zone and to the unaffected base metal during and after welding, a non-uniform hydrogen concentration exists. This migration of hydrogen also increases the active anodic area and invalidates the assumption of uniform  $C_0$  in the Gileadi planar-diffusion model.

Other factors may have contributed to the discrepancy between the Gileadi-model transient and the measured transients. The current obtained from the control specimen might have been derived from hydrogen oxidation as a result of liberation of residual hydrogen. The control transient might also reflect corrosion currents or some other competing surface reaction that produced electrons.

#### Spherical Decanted Weld Specimens

A spherical shape was chosen for testing to alleviate the geometry and active, anodic area problems. Round specimens could be produced by existing weld-metal decanting techniques. In addition, the diffusion of hydrogen could be simply modeled in a spherical specimen.

Decanted weld specimens were made utilizing HY-130 base plate and E-14018 SMAW electrodes. The specimens diameters were approximately 0.48 cm for decant Specimen No. 1 and

0.52 cm for Specimen No. 2.

Corrosion potentials, which were measured 60 seconds after immersion in the electrolyte, were approximately -1000-mv (S.C.E.) for both specimens. Each decant was tested for one hour in the Barnacle Cell. The measured current-time transients for the decanted weld specimens are shown in Figure 12.

The lower curve in Figure 12, labelled S, is a computed current-time transient, which was generated from the Fourier-transform, spherical-diffusion solution:

$$I_A = 8\pi r_0 D F C_0 \sum_{n=1}^{\infty} \exp\left(\frac{-n^2 \pi^2 D t}{r_0^2}\right)$$

In computing the current values, the specimen radius,  $r_0$ , was assumed to be 0.25 cm, the average for decant Specimens 1 and 2. The diffusivity,  $D$ , which is unknown, was assumed to be  $4.0 \times 10^{-7} \text{ cm}^2/\text{sec}$ , in accordance with the value reported by Berman for hydrogen in HY-130 weld metal.<sup>(Ref.6)</sup> A change in the value of  $D$  employed would change both the position and the shape of Curve S. However, a change in the assumed initial hydrogen content,  $C_0$ , would change only the vertical position of Curve S. This is because the diffusion solution is linear in  $C_0$  and Figure 12 is a logarithmic plot.

The value of  $C_0$  assumed in plotting Curve S was  $3.9 \times 10^{-5}$  moles of diffusible hydrogen per  $\text{cm}^3$  of weld-metal, which corresponds to a hydrogen level of 5.0 ppm on a weight basis. This value was selected from hydrogen-content data, obtained

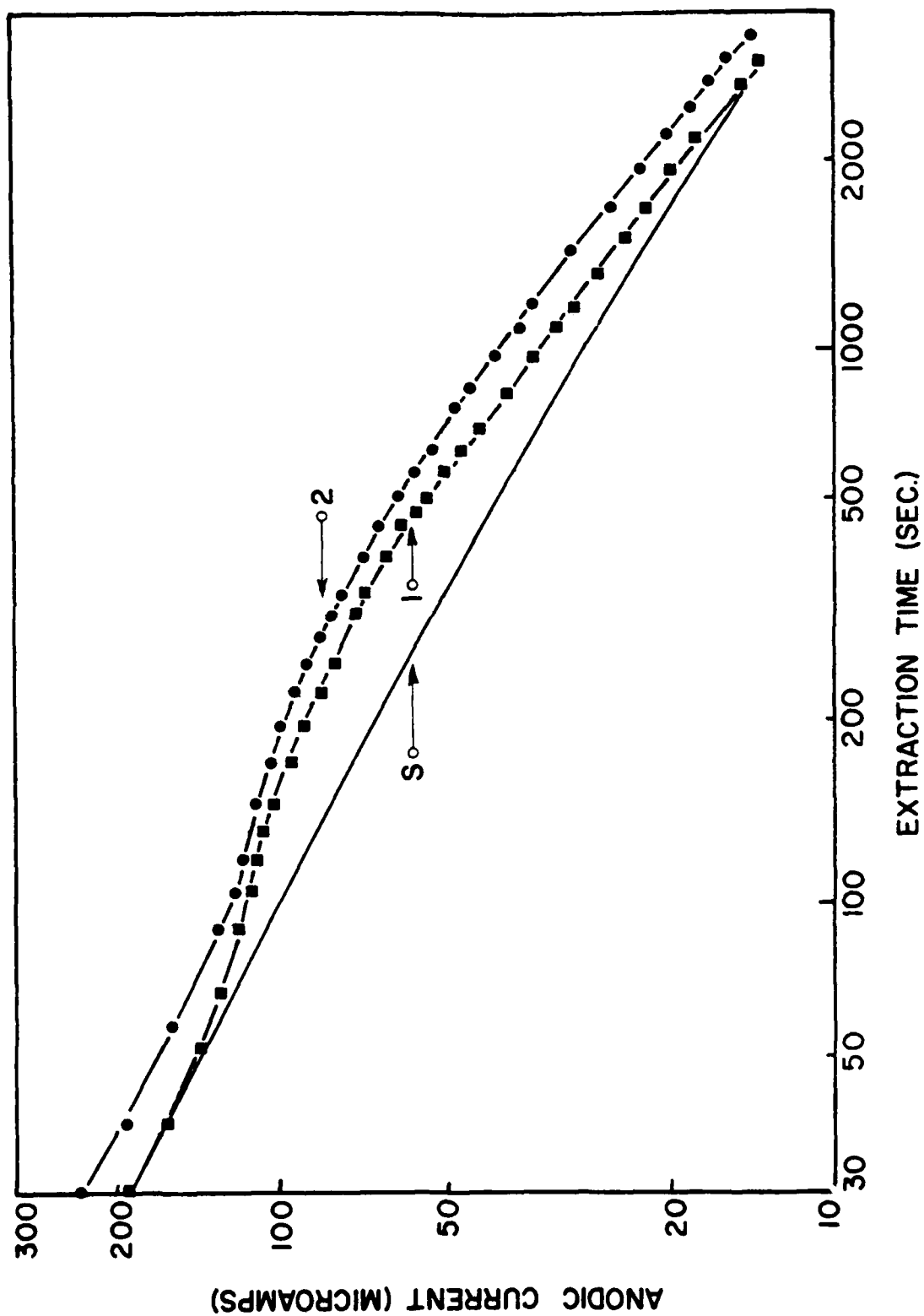


Figure 12. Extraction Transients from Decant Weld Specimens.



by the IIW/BWRA method, for the welding parameters utilized. In computing Curve S, the infinite series in the diffusion solution was terminated when the value of the succeeding term was less than 0.001.

As illustrated in Figure 12, the calculated transient S shows poor agreement with the experimental transients for Specimen No. 1 and No. 2. This lack of congruence suggests that the diffusion model is not applicable to the extraction of hydrogen from weld-metal decant specimens.

The failure in the application of the diffusion model may have been related to the random-burst bubble evolution that was observed during testing and to specimen cracking. The decanted specimens were sectioned metallographically to determine the source of the bubble evolution and the existence of cracking. Examination of decant cross-sections revealed macropores and extensive intergranular cracking at the periphery of the specimens. The cracks were narrow, showed some branching, and had the morphology of quench-induced and/or hydrogen-induced cracking.

The cracks could have influenced the Barnacle-Cell transients in several ways. If the cracks are at the surface of a specimen, additional anodic area for the oxidation reaction is provided. The irregular shape of this additional surface would violate the assumption of spherical symmetry in the diffusion solution. Both the additional anodic area and the violation of symmetry would be expected to increase the extraction rate over that predicted by the spherical-

diffusion model. In Figure 12 the slopes of both measured transients are, except for short times, steeper than Curve S. These steeper slopes confirm the presence of a higher-than-predicted extraction rate.

Narrow surface cracks could also introduce contaminants into the test cell, such as: welding flux, moisture, ethanol quenchant, or air which could be trapped in the cracks. The presence of trapped oxygen could lead to crevice corrosion, which would cause only local currents. However, the availability of oxygen could also cause general corrosion. This general dissolution would produce anodic current in the external circuit. Currents might also be caused by entrapped organic contaminants. The organic molecules could compete with the diffusing hydrogen for anodic sites on the surface.

#### Steel-Shot Specimens

In order to eliminate the effect of cracks in weld-decant specimens on the extraction currents, spherical low-carbon-steel shot specimens were used for testing in the modified Barnacle Cell. The specimens were prepared by charging in a hydrogen atmosphere at 955°C.

The specimens used in the first group of tests were cleaned after hydrogen-charging by grit blasting with 10- $\mu$ m alundum. Preparation conditions employed for these specimens are shown in Table 8. A second group of specimens was pre-cleaned and, after hydrogen charging, was quenched

Preparation Conditions and Corrosion Potentials  
for Hydrogen-Charged, Blast-Cleaned, Steel-Shot Specimens

TABLE 8

Furnace Run Number	Charging Temperature °C	Charging Time* Hours	Average Corrosion Potential S.C.E., mv.	
			Initial	Final**
1	925	0.5	-830	-540
2	955	0.5	-800	-400
3	955	0.7	-790	-400
4	955	0.6	-820	-380
5	955	0.7	-800	-390

\*Charging time includes the time, which is less than 5 minutes, for specimens to reach charging temperature.

\*\*Final corrosion potential measured after 3600 seconds.

in a dry ice-alcohol mixture ( $-70^{\circ}\text{C}$ ,  $-94^{\circ}\text{F}$ ) which was contained within a non-oxidizing atmosphere. Preparation conditions for these specimens are shown in Table 9.

The published value of the solubility limit of hydrogen in iron at  $955^{\circ}\text{C}$  is 4.5 ppm. However, the results of analyses of the hydrogen-charged steel shot by the BWRA/IIW test procedure and the RPI Silicone-Oil Extraction Method (to be discussed in the third portion of this report) indicated that the hydrogen content was dependent on the charging time. For a charging time of 1/2 hour at  $955^{\circ}\text{C}$ , a diffusible hydrogen content of 1.51 ppm was measured, as shown in Table 10. The hydrogen content increased asymptotically to 2.27 ppm after 4 hours of charging at  $955^{\circ}\text{C}$ . In addition, hydrogen-content data for  $925^{\circ}$  and  $905^{\circ}\text{C}$  charging temperatures are included in Table 10. It is to be noted that the steel shot was in the cold-worked condition when placed in the hydrogen-charging furnace. Thus, equilibration of the structure and composition of the steel shot required several hours exposure to the heat treatment temperature and atmosphere.

Hydrogen-free control specimens were produced by degassing in a vacuum furnace at approximately  $1050^{\circ}\text{C}$ . Uncharged specimens were also used for comparison purposes.

Computed Transients. Extraction-current transients were computed for diffusivity values ranging from  $10^{-8}$  to  $10^{-5}\text{cm}^2/\text{sec}$ . The transients were generated from the

TABLE 9

Preparation Conditions and Corrosion Potentials  
for Hydrogen-Charged, Steel-Shot Specimens  
Quenched Within a Non-Oxidizing Atmosphere

Furnace Run Number	Pre-Charge Pickling	Charging Temperature* °C	Charging Time Hours	Non-Oxid. Atmosphere	Average Corrosion Potential S.C.E., mv.	
					Initial	Final
6	None	955	1	Ar	-970	-380
7	None	955	0.5	Ar	-920	-600
8	None	955	0.5	Ar	-940	-580
9	50% HCl 30 seconds	955	0.5	N <sub>2</sub>	-910	-530
10	50% HCl 20 seconds	905	5.2	N <sub>2</sub>	-850	-530
11	50% HCl 60 seconds	955	3.7	N <sub>2</sub>	-920	-400
12	50% HCl 120 seconds	955	3.2	Ar	-870	-470

\*Charging time includes the time, which is less than 5 minutes, for specimens to reach charging temperature.

\*\*Final corrosion potential measured after 3600 seconds.

TABLE 10  
Diffusible Hydrogen Content  
of Steel-Shot Specimens

<u>Charging Time Hours</u>	<u>Charging Temp. °C</u>	<u>Average Hydrogen Content, ppm</u>	
		<u>Silicone-Oil Method</u>	<u>BWRA/IIW Method</u>
1/2	955	1.51 $\pm$ 0.25*	1.34
1	955	1.73 $\pm$ 0.23	1.71
2	955	1.90 $\pm$ 0.43	1.95
4	955	2.27 $\pm$ 0.35	-
2	925	1.26 $\pm$ 0.28	-
4	905	1.26 $\pm$ 0.43	-

\* The data reported include the calculated standard-deviation values for at least 8 determinations.

Fourier-transform, spherical-diffusion solution:

$$I_A (\mu a) = \frac{8\pi r_0 D C_0 z F \rho}{M} \sum_{n=1}^{\infty} \exp\left(-\frac{n^2 \pi^2 D t}{r_0^2}\right).$$

The steel density,  $\rho$ , 7.87 g/cm<sup>3</sup>, and the atomic weight,  $M$ , of dissolved hydrogen, 1.008 g/mole, have been included to permit expressing  $C_0$  in ppm. The valence,  $z$ , is 1.0 equivalent of charge per mole of dissolved hydrogen which has been oxidized. The Faraday constant,  $F$ , is 96,487 coulombs/equivalent, and the specimen radius,  $r_0$ , has been assumed to be 0.162 cm. Assuming a  $C_0$  value of 4.5 ppm, current values were computed from the diffusion solution for various values of  $D$  and for extraction times of 30 to 6000 seconds. Table 11 summarizes the results of these computations, and calculated transients for 7 different values of  $D$  are plotted in Figure 13.

To estimate the diffusible-hydrogen content,  $C_0$ , of a specimen, the measured extraction transient is curve-matched at a specific time to a computed transient which corresponds to a particular value of  $D$  and a  $C_0$  value of 4.5 ppm. During the curve-matching process, the vertical positions of the calculated curve may be changed because the intercept value is dependent on  $C_0$ . The estimated  $C_0$  value may be determined from:

$$\frac{\text{Estimated } C_0}{4.5} = \frac{\text{Measured } I_A}{\text{Computed } I_A}$$

TABLE 11  
Calculated Extraction Currents\*

Time (secs.)	Diffusivity, $\text{cm}^2/\text{sec.}$					
	$1 \times 10^{-8}$	$4 \times 10^{-8}$	$1 \times 10^{-7}$	$4 \times 10^{-7}$	$1 \times 10^{-6}$	$4 \times 10^{-6}$
30	11.4	23	35.8	70	108	203
60	8.0	16.0	25.0	43.8	74.6	135
120	5.7	11.2	17.6	33.6	50.6	87.6
180	4.6	9.2	14.2	27.0	40.2	66.4
360	3.6	7.0	10.8	20.2	29.6	45.2
420	3.0	5.8	9.0	16.8	23.8	34.0
600	2.51	4.8	7.4	13.6	18.8	24.0
900	2.03	3.9	6.0	10.6	14.2	14.6
1200	1.75	3.4	5.0	8.8	11.4	9.2
1500	1.56	3.0	4.4	7.6	9.4	5.8
1800	1.42	2.7	4.0	6.6	8.0	3.7
2100	1.31	2.5	3.6	6.0	6.8	2.34
2400	1.22	2.3	3.4	5.4	6.0	1.49
3000	1.08	2.02	2.96	4.6	4.6	0.606
3600	0.982	1.82	2.64	3.88	3.62	0.24
4200	0.904	1.67	2.35	3.40	2.86	0.097
6000	0.745	1.36	1.88	2.40	1.44	$7 \times 10^{-3}$
						$2 \times 10^{-3}$
						$2 \times 10^{-4}$
						$2 \times 10^{-5}$
						$2 \times 10^{-8}$

\*Values of extraction current,  $I_A$  in microamperes, as a function of time for spherical specimens with  $C_0=4.5\text{ppm}$  for different values of  $D$ , diffusivity.



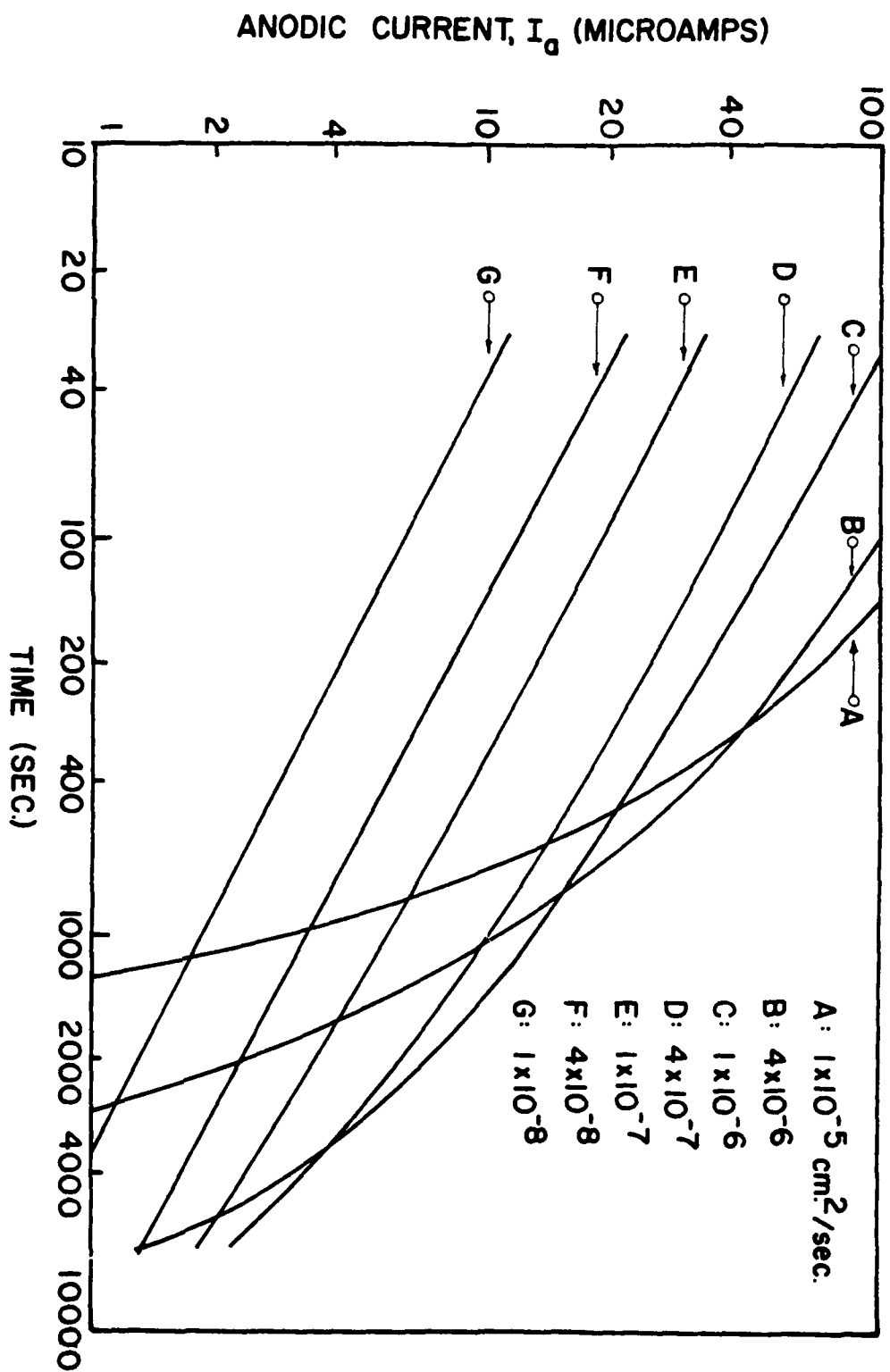


Figure 13. Computed Extraction Transients Utilizing Various Values of Diffusivity, D, for Spherical Specimens.

The Computed  $I_A$  is found in either Table 11 or Figure 13 for the specific value of  $D$  at which curve matching was accomplished and for the specific value of time at which the Measured  $I_A$  was determined.

The precision of the estimated  $C_0$  value is limited by the accuracy of the curve-matching process. Unfortunately, the shapes of the computed transients are not strongly dependent on the value of the diffusion coefficient. As shown in Figure 13, the transients are nearly parallel with diffusivities of  $1 \times 10^{-7}$ ,  $4 \times 10^{-8}$ , and  $1 \times 10^{-8} \text{ cm}^2/\text{sec}$ . (Curves E, F, and G) for extraction times up to 1000 seconds. Even for a  $D = 10^{-6} \text{ cm}^2/\text{sec}$ . (Curve C), the transient is nearly parallel to the lower curves for the first 600 seconds. Thus, matching should not be attempted at small values of time.

Effect of Lead Wires. To determine the contribution of the steel lead wires to the extraction-current transients, lead wires from several hydrogen-charged specimens in Run 11 were tested in the modified Barnacle Cell after detachment from the steel shot. As may be seen in Table 12, the ratio of the average lead-wire extraction current to the average extraction current for shot specimens with lead wires attached increased from 0.17 at 30 seconds to 0.39 at 600 seconds, after which the ratio remained constant. These results are reasonable in view of the

TABLE 12

Comparison of Extraction Currents,  $I_A$  in Microamperes,  
From Lead Wires and From Shot Specimens With Lead Wires

Condition	Extraction Time-secs.								
	30	60	120	240	480	600	900	1200	1920
Lead Wire	17.2	11.8	8.9	6.3	4.6	3.9	2.77	2.23	1.51
Lead Wire & Specimen	100	64	37	21	12	10.0	7.1	5.7	3.9
Specimen	82.8	52.2	28.1	14.7	7.4	6.1	4.33	3.47	2.39
Ratio of Extraction Currents:	0.172	0.184	0.24	0.30	0.383	0.39	0.39	0.39	0.39

Wire  
Wire & Specimen

fact that the volume of the lead wire which is immersed in the electrolyte is approximately 30% of the combined volume of the shot and the wire. In addition, the surface area of the immersed portion of a lead wire is almost twice that of a spherical shot specimen.

In order to adjust for the effect of a lead wire, each measured transient was corrected by subtracting the portion of the extraction-current transient contributed by the lead wire. A typical example of this correction procedure is shown in Figure 14. It should be noted that subtraction of the lead-wire current from the total current results in a change of slope in the extraction current for the shot specimen.

Measured Extraction Current Transients for Grit-Blasted Specimens. The three extraction-current transients, labelled #1, #2, and #3 in Figure 15, were obtained from Specimens 1, 2, and 3, respectively, from Furnace Run 1. Note that these transients are concave upward, whereas the computed transients in Figure 13 are concave downwards. Obviously, it is impossible to curve-match the measured and computed transients for long-time intervals. Therefore, it is necessary to curve-match the measured transients with the computed transients for short intervals at long extraction times.

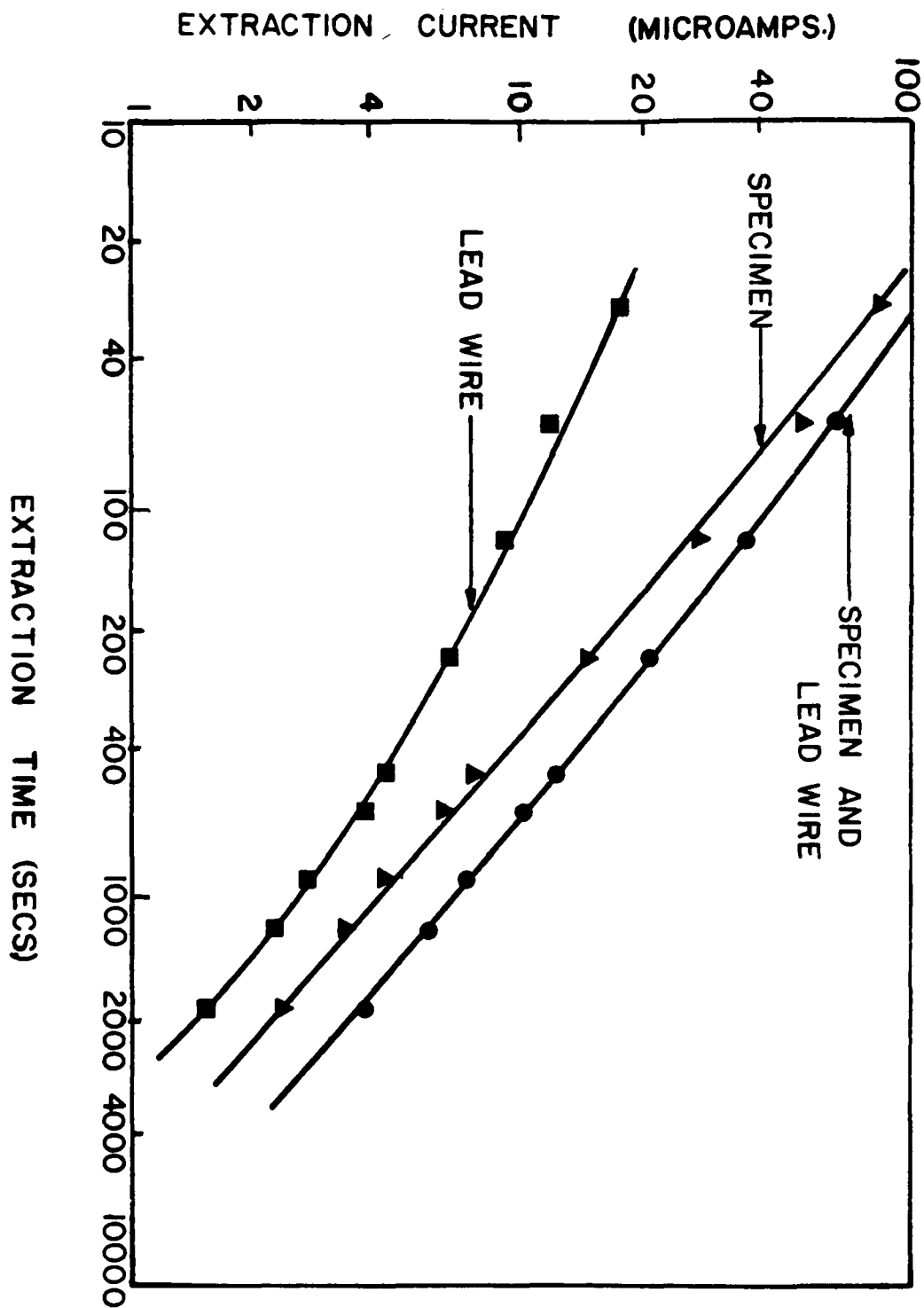


Figure 14. The Effect of Lead Wires on Measured Extraction Transients.

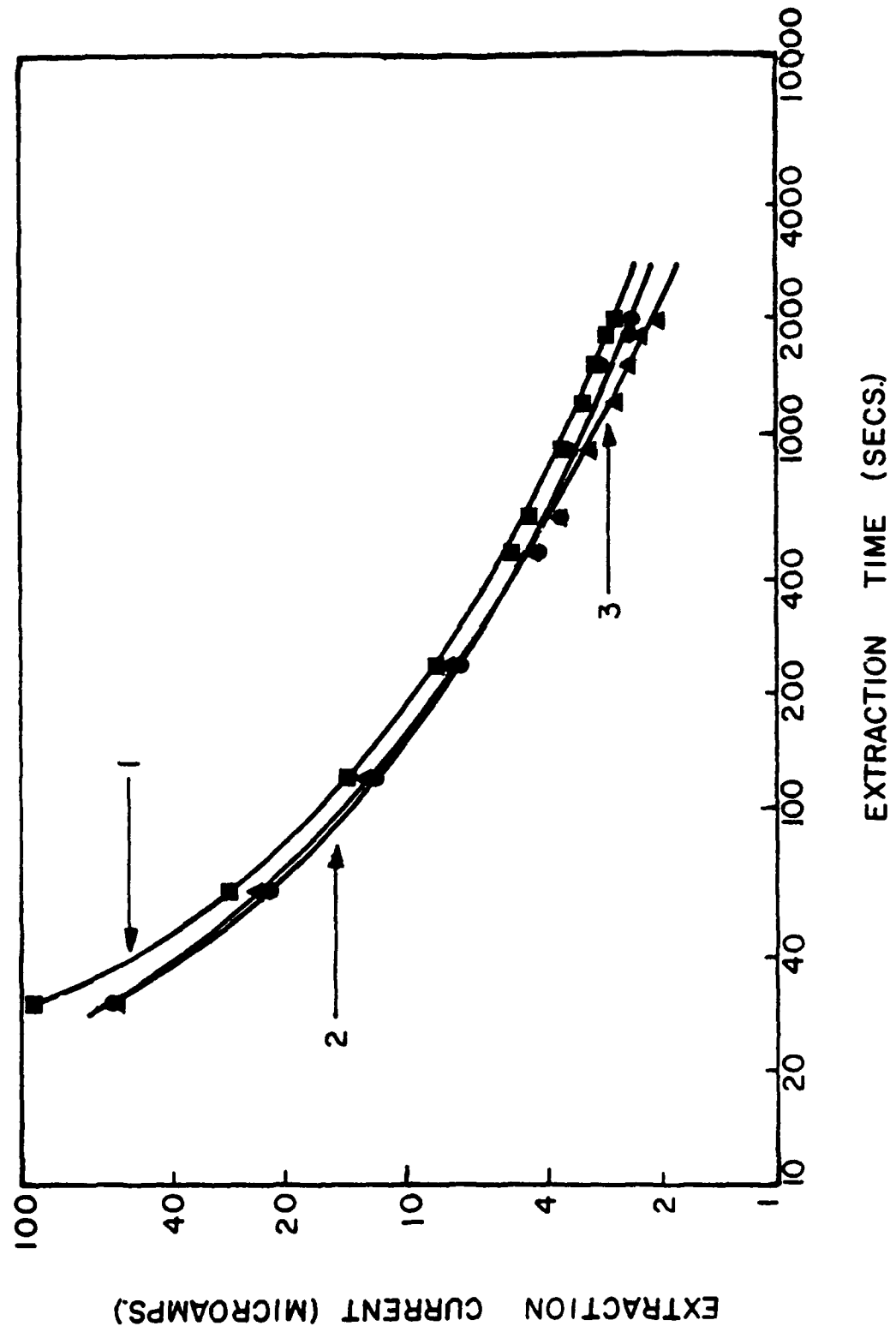


Figure 15. Extraction Transients from Run 1, Steel-Shot Specimens.

For example, in Figure 15, the uppermost transient, which was obtained from Shot No. 1 of Furnace Run 1, corresponds to a computed transient with a  $D$  value of approximately  $1 \times 10^{-6} \text{ cm}^2/\text{sec.}$  for  $180 < t < 420 \text{ sec.}$ , at an estimated  $C_0$  of 0.95 ppm, whereas in the time interval from 1500 to 2000 seconds the  $D$  value is approximately  $4 \times 10^{-8} \text{ cm}^2/\text{sec.}$  with an estimated  $C_0$  of 4.47 ppm. Transient 2 in Figure 15 can be curve-matched for  $180 < t < 420$  seconds, although the fit is poorer than in the previous case. The best correlation is obtained with  $D = 2 \times 10^{-6} \text{ cm}^2/\text{sec.}$  and an estimated  $C_0$  of 0.62 ppm. In the time interval from 1200 to 2000 seconds  $D$  is  $4 \times 10^{-7} \text{ cm}^2/\text{sec.}$  with  $C_0$  equal to 1.67 ppm. Transient 3 is matched with  $D = 4 \times 10^{-6} \text{ cm}^2/\text{sec.}$  in the range of  $180 < t < 420$  seconds, which corresponds to a  $C_0$  value of 0.55 ppm, and with  $D = 1 \times 10^{-7} \text{ cm}^2/\text{sec.}$  in the time interval 1200 to 2000 seconds, which corresponds to  $C_0 = 2.5 \text{ ppm.}$

It should be noted that the diffusivity values in the 1200- to 2000-second intervals for the specimens from Run 1 were different. The remainder of the grit-blasted, hydrogen-charged specimens (Runs 2-5) also exhibited a variation in  $D$  values from specimen to specimen and from run to run.

As shown in Table 13, the diffusivity values,  $D$ , appear to vary from  $1 \times 10^{-8}$  to  $1 \times 10^{-6} \text{ cm}^2/\text{sec.}$  among the specimens tested. The estimated  $C_0$  values for the specimens

TABLE 13

Estimated Diffusible Hydrogen Content (ppm) and  
Diffusivity Values for Hydrogen-Charged, Grit-Blasted Specimens

Specimen Number	Furnace Run Number				
	<u>1</u>	<u>2</u>	<u>3</u>	<u>4</u>	<u>5</u>
1	4.5 ( $4 \times 10^{-8}$ )*	2.2 ( $1 \times 10^{-7}$ )	1.6 ( $1 \times 10^{-7}$ )	1.7 ( $4 \times 10^{-8}$ )	1.7 ( $1 \times 10^{-7}$ )
2	1.7 ( $4 \times 10^{-7}$ )	1.7 ( $1 \times 10^{-7}$ )	0.7 ( $4 \times 10^{-7}$ )	1.25 ( $1 \times 10^{-7}$ )	0.9 ( $4 \times 10^{-7}$ )
3	2.5 ( $1 \times 10^{-7}$ )	1.85 ( $1 \times 10^{-7}$ )	1.5 ( $1 \times 10^{-7}$ )	2.3 ( $1 \times 10^{-8}$ )	0.6 ( $1 \times 10^{-6}$ )
4	--	--	1.5 ( $1 \times 10^{-7}$ )	--	2.6 ( $4 \times 10^{-8}$ )
Run Average	2.90	1.92	1.33	1.75	1.45
Extraction Analysis	1.43	1.51	1.61	1.56	1.61

\*Data in parentheses correspond to estimated values of Diffusivity,  $\text{cm}^2/\text{sec}$ ,  
in the time interval between 1200 and 2000 seconds.



in Runs 1-5, utilizing the appropriate D values, are also summarized in Table 13. The variation in D values results in a large range of diffusible-hydrogen contents,  $C_0$ , within each run.

Assuming that D is  $1 \times 10^{-7} \text{ cm}^2/\text{sec.}$  for the specimens tested, the range of diffusible hydrogen contents of the specimens is very reasonable. These  $C_0$  values for Runs 1-5 are shown in Table 14.

As shown in Tables 13 and 14, the average diffusible hydrogen contents of Runs 1-5, as determined by the modified Barnacle Cell technique, were comparable to those determined utilizing the BWRA/IIW and RPI Silicone Oil Extraction methods. The correspondence of diffusible hydrogen contents is better when a value of D of  $1 \times 10^{-7} \text{ cm}^2/\text{sec.}$  is selected in the Barnacle Cell technique, as illustrated in Table 14.

Measured Extraction Current Transients for Specimens Quenched in a Non-Oxidizing Atmosphere. To avoid the possible loss of hydrogen during grit blasting, extraction transients were measured for hydrogen-charged specimens which were quenched in a dry ice-alcohol bath contained within a non-oxidizing atmosphere. No bubble evolution was detected from any of the specimens and quench cracking was not observed.

TABLE 14

Estimated Diffusible Hydrogen Content\* (ppm) for  
Hydrogen-Charged Grit-Blasted Specimens

Spec. No.	Furnace Run Number				
	<u>1</u>	<u>2</u>	<u>3</u>	<u>4</u>	<u>5</u>
1	2.8	2.2	1.6	1.2	1.7
2	2.75	1.7	1.25	1.25	1.5
3	2.5	1.85	1.5	1.6	1.3
4	-	-	1.5	-	1.8
Run Average	2.68	1.92	1.46	1.35	1.58
Extraction Analysis	1.43	1.51	1.61	1.56	1.61

\*Diffusible-hydrogen content with  $D = 1 \times 10^{-7}$  cm<sup>2</sup>/sec. at 1200 seconds.

The extraction transients of the steel shot, which were quenched in a non-oxidizing atmosphere resembled those of the grit-blasted specimens. In addition, the  $D$  values varied from specimen to specimen as they did in the grit-blasted specimens. Table 15 summarizes the diffusivity values and the diffusible-hydrogen content of the specimens from hydrogen-charged Runs 6-12 utilizing these  $D$  values.

The large variation in  $C_0$  of the specimens from a particular hydrogen-charging run is reduced significantly by using a common value of  $D$  for calculating the diffusible-hydrogen content,  $C_0$ . The  $C_0$  values for Runs 6-12, utilizing  $D=1 \times 10^{-7} \text{ cm}^2/\text{sec.}$ , are listed in Table 16.

As may be noted from Tables 15 and 16, the correspondence between the hydrogen contents measured by the Barnacle Cell technique and those measured by extraction methods is good. The correspondence is somewhat better when  $D$  of  $1 \times 10^{-7} \text{ cm}^2/\text{sec.}$  is used in the Barnacle Cell technique, as shown in Table 16.

#### Sensitivity Analysis

If the diffusion solutions are examined mathematically, an insight into the sensitivity of the solution to parameter errors may be developed. In the case of spherical specimens, a fractional error in the value of  $D$ , will result in a fractional error of the same magnitude

TABLE 15

Estimated Diffusible Hydrogen Content (ppm) and  
Diffusivity Values for Hydrogen-Charged Specimens  
Quenched Within a Non-Oxidizing Atmosphere

Specimen Number	Furnace Run Number						
	<u>6</u>	<u>7</u>	<u>8</u>	<u>9</u>	<u>10</u>	<u>11</u>	<u>12</u>
1	0.9 ( $1 \times 10^{-6}$ )*	1.7 ( $4 \times 10^{-8}$ )	1.35 ( $1 \times 10^{-7}$ )	1.2 ( $1 \times 10^{-7}$ )	0.8 ( $1 \times 10^{-7}$ )	1.6 ( $1 \times 10^{-6}$ )	2.6 ( $4 \times 10^{-8}$ )
2	1.0 ( $1 \times 10^{-6}$ )	1.9 ( $4 \times 10^{-8}$ )	4.0 ( $1 \times 10^{-8}$ )	1.0 ( $1 \times 10^{-8}$ )	3.2 ( $1 \times 10^{-8}$ )	1.6 ( $1 \times 10^{-6}$ )	-
3	0.9 ( $4 \times 10^{-7}$ )	1.9 ( $4 \times 10^{-8}$ )	0.5 ( $1 \times 10^{-6}$ )	1.3 ( $1 \times 10^{-8}$ )	0.5 ( $1 \times 10^{-6}$ )	1.3 ( $1 \times 10^{-6}$ )	3.25 ( $4 \times 10^{-8}$ )
4	0.7 ( $1 \times 10^{-7}$ )	1.7 ( $4 \times 10^{-8}$ )	0.5 ( $1 \times 10^{-6}$ )	4.0 ( $1 \times 10^{-8}$ )	0.5 ( $1 \times 10^{-6}$ )	1.25 ( $1 \times 10^{-6}$ )	1.95 ( $4 \times 10^{-8}$ )
Run Average	0.87	1.80	1.59	1.87	1.25	1.44	2.60
Extraction Analysis	1.73	1.51	1.51	1.51	1.26	2.27	2.15

\*Data in parentheses correspond to estimated values of Diffusivity,  $\text{cm}^2/\text{sec}$ ,  
in the time interval 1200 to 2000 seconds.

TABLE 16

Estimated Diffusible Hydrogen Content\* (ppm)  
For Hydrogen-Charged Specimens  
Quenched Within a Non-Oxidizing Atmosphere

<u>Specimen Number</u>	<u>Furnace Run Number</u>					
	<u>6</u>	<u>7</u>	<u>8</u>	<u>9</u>	<u>10</u>	<u>11</u>
1	1.9	1.2	1.3	1.2	1.35	3.4
2	2.1	1.3	1.4	1.4	1.1	3.4
3	1.6	1.3	1.1	0.9	1.2	2.8
4	1.5	1.2	1.1	1.4	1.2	2.7
Run Average	1.77	1.25	1.23	1.23	1.21	3.07
Extraction Analysis	1.73	1.51	1.51	1.51	1.26	2.27
						2.15

\*Diffusible-hydrogen content with  $D = 1 \times 10^{-7} \text{ cm}^2/\text{sec.}$  at 1200 seconds.

in  $C_0$ . Unfortunately, it is difficult to obtain a reliable value for  $D$  at room temperature. Different authors, using various measuring techniques, have reported values varying by as much as 3 orders of magnitude for the same material.<sup>(Ref.15)</sup> Even where one measuring technique is used consistently, the precision obtained is not high. For example, Berman reported a diffusivity of  $(4.0 \pm 2.2) \times 10^{-7} \text{ cm}^2/\text{sec.}$  at 95% confidence for HY-130 weld metal.<sup>(Ref.6)</sup> If there is an uncertainty of  $\pm 50\%$  in the nominal value of  $D$ , then there will be an uncertainty of at least  $\pm 50\%$  in the values of  $C_0$ . This assumes that the Barnacle transient is a perfect match to the diffusion solution.

In the diffusion solution for rectangular specimens,  $C_0$  is proportional to  $D^{1/2}$ . In this case, if there is an uncertainty of  $\pm 50\%$  in the value of  $D$ , then the uncertainty in the value of  $C_0$  would correspond to  $+22\%$  and  $-30\%$ .

The solution to any diffusion model will, of necessity, be sensitive to the value of  $D$ . To utilize the modified Barnacle Cell as a diffusible-hydrogen measuring device, requires matching of the transients of a diffusion solution which is sensitive to the value of  $D$ . Therefore, the accuracy of determining diffusible-hydrogen content by this device is limited by the ability to estimate  $D$ , accurately.

### Vacuum-Degassed Steel Shot

To aid in characterizing the effect of competing anodic reaction(s) on the extraction current, both hydrogen-free and uncharged specimens were produced and tested in the modified Barnacle Cell. The hydrogen-free specimens were prepared by hot vacuum degassing for 1 hour at approximately 1050°C. The specimens were stored in liquid N<sub>2</sub> to prevent diffusive pickup and had a H<sub>2</sub> content estimated to be approximately 10<sup>-3</sup> ppm.

Figure 16 is a comparison of the average extraction transient from seven vacuum-degassed, steel-shot specimens, the extraction transient from an uncharged steel-shot specimen, and the average extraction transient of the hydrogen-charged, steel-shot specimens from Run 1. The current obtained from the vacuum-degassed specimens is negligible,  $I_A < 0.1 \mu A$ . A change in extraction current of this magnitude would have a very minor effect on the determination of the diffusible-hydrogen content,  $C_0$ , of a hydrogen-charged specimen. For example, the contribution to the  $C_0$  value of a hydrogen-charged specimen resulting from a change in the extraction current,  $I_A$ , of  $\pm 0.012 \mu A$  at 1200 seconds with a  $D$  of  $1 \times 10^{-7} \text{ cm}^2/\text{sec}$ . would be  $\pm 0.01$  ppm.

In addition, the extraction current from the uncharged steel shot was  $0.65 \mu A$  at 1200 seconds with a  $D$  of  $2 \times 10^{-6} \text{ cm}^2/\text{sec}$ ., this corresponds to a diffusible-hydrogen

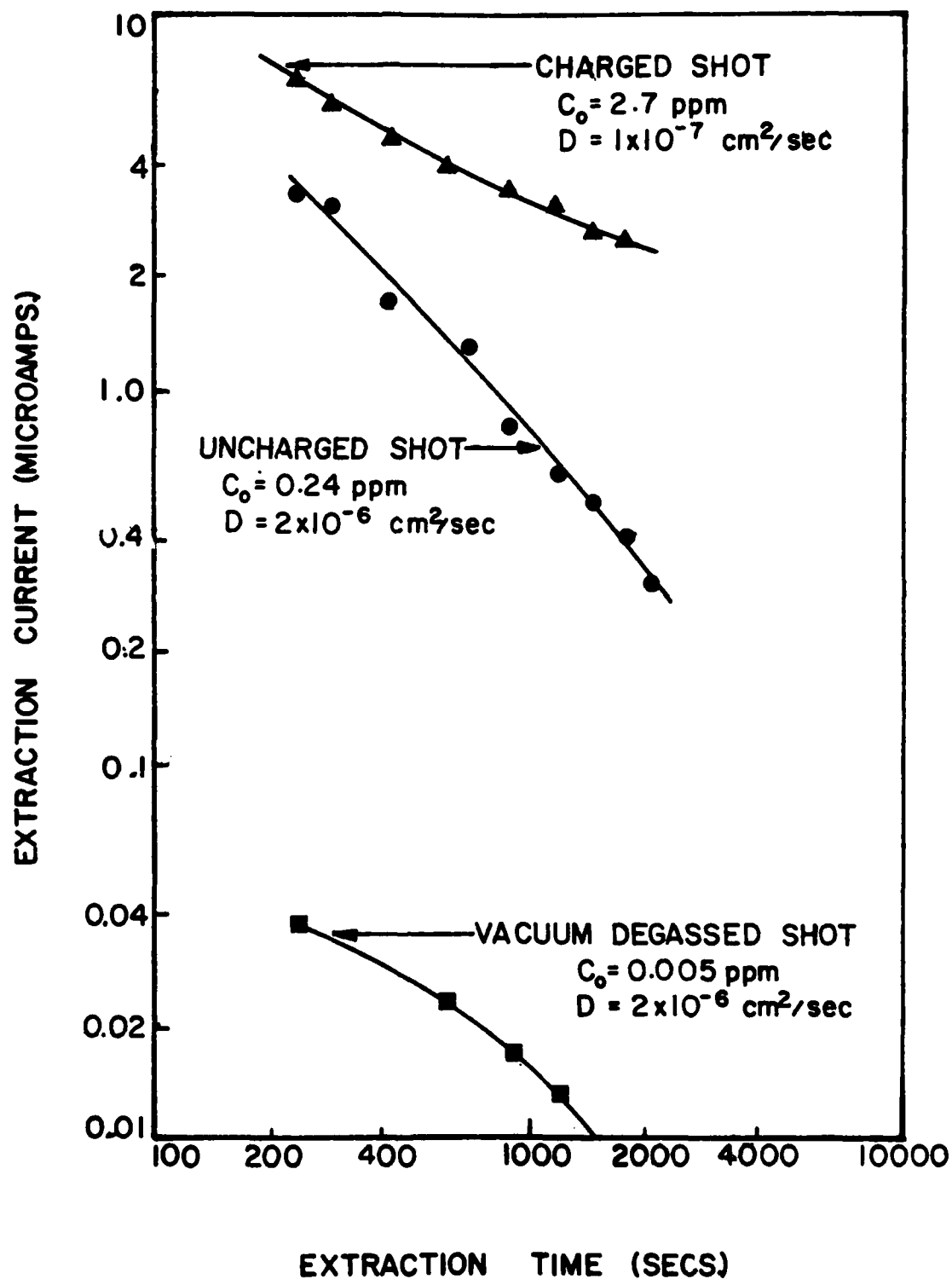


Figure 16. Extraction Transients from Charged, Uncharged, and Vacuum Degassed Steel-Shot Specimens.



content of 0.24 ppm. This  $C_0$  value for the uncharged steel shot is reasonable because the specimen was pickled for 30 seconds in 50% HCl, before testing. These data also confirm the results reported by Berman, et al. for the original Barnacle Cell. (Ref.6) In those tests, welds and cathodically charged specimens produced currents two to ten times greater than the transients of uncharged plate specimens. Thus, competing anodic reactions did not have a significant effect on the extraction currents obtained from specimens tested in the modified Barnacle Cell.

#### SUMMARY

The modified Barnacle Cell could not be used to determine the diffusible hydrogen content of rectangular bead-on-plate specimens because the diffusion model for rectangular specimens is not applicable to bead-on-plate specimens; the weld bead results in a non-rectangular geometry and a non-uniform hydrogen content.

When weld-decant specimens were utilized as a source for hydrogen analysis, it was discovered that the samples contained cracks which affected the extraction currents. These cracks supplied additional anodic area and provided a means of introducing contaminants into the modified Barnacle Cell.

The study of spherical, hydrogen-charged specimens indicates that the modified Barnacle Cell measures the current obtained from the oxidation of hydrogen extracted from a specimen without significant current being generated by competing anodic reactions. However, the determination of diffusible hydrogen content,  $C_O$ , from the extraction current,  $I_A$ , is limited by the ability to estimate, accurately, the diffusivity,  $D$ . Unfortunately, as mentioned previously, the value of  $D$  at room temperature cannot be measured with high precision. The room-temperature value of  $D$  is quite sensitive to such factors as: the chemical composition, grain size, microstructure, dislocations, inclusions, and microvoids of the steels.<sup>(Ref.15)</sup>

## THE RPI SILICONE-OIL EXTRACTION METHOD

This method involves the extraction of diffusible hydrogen from a sample placed in hydrogen-saturated silicone oil at 100°C and the subsequent collection of this hydrogen in a burette. Because the extraction is performed at an elevated temperature, the test time required is short, approximately 1 1/2 hours.

### Apparatus

Figure 17 is a schematic illustration of the apparatus used in the RPI method. The apparatus consists of two pyrex beakers set up in a "double-boiler" bath configuration, heated by a standard laboratory hot plate. Both the inner and outer baths are a standard high-grade, high-temperature, silicone oil which is stable up to 200°C (392°F). The inner bath is maintained at a constant temperature, 100°C  $\pm$  5°C. The double-boiler arrangement eliminates any hot spots between the specimen and the base of the inner bath. A test temperature of 100°C has been established because it provides an incubation time which is sufficient to enable the specimen to be positioned under the collection funnel before evolution of hydrogen begins. At higher temperatures, gas evolution begins before the specimen can be maneuvered under the funnel. Also, at temperatures greater than 100°C hydrogen evolution is so rapid that a froth develops at the meniscus in the burette and, therefore,

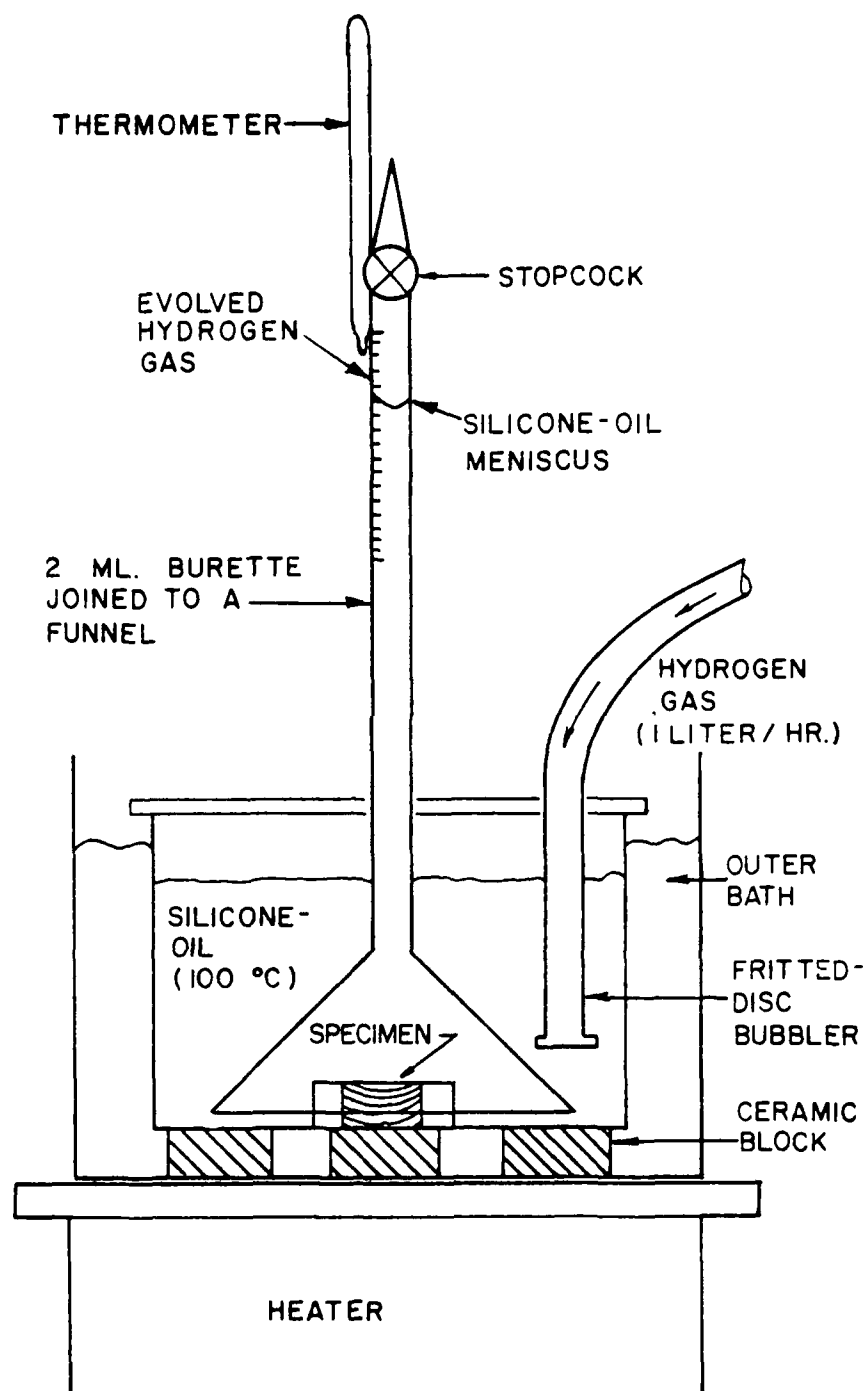


Figure 17. Diagram of RPI Silicone-Oil Apparatus.

renders measurement impossible until the froth of bubbles disappears and a true meniscus re-forms.

The inner bath is maintained saturated with hydrogen by bubbling hydrogen directly into the bath through a fritted-disc bubbler of pore size E, 4-8 $\mu$ m, at a constant flow rate of approximately 1 liter/hour. By maintaining a saturated solution, all of the diffusible hydrogen evolved from a specimen is collected; none is lost by solution into the silicone-oil bath.

The final component of the RPI apparatus is a pyrex collection funnel which is attached to a 2-ml calibrated burette. Silicone oil is drawn up the column such that the meniscus is in the calibrated portion of the burette. The specimen is placed under this collection funnel. The evolved hydrogen rises to the top of the silicone-oil column and is trapped in the burette. The entire apparatus is pictured in Figure 18.

An additional advantage of the RPI system is its adaptability. Variable specimen size can be accommodated by merely scaling up the entire apparatus.

#### Calibration

After the equipment has been assembled, the temperature has equilibrated to 100°C, and the silicone-oil has become saturated with hydrogen, the initial hydrogen volume must be established. This is achieved by a two-step process:

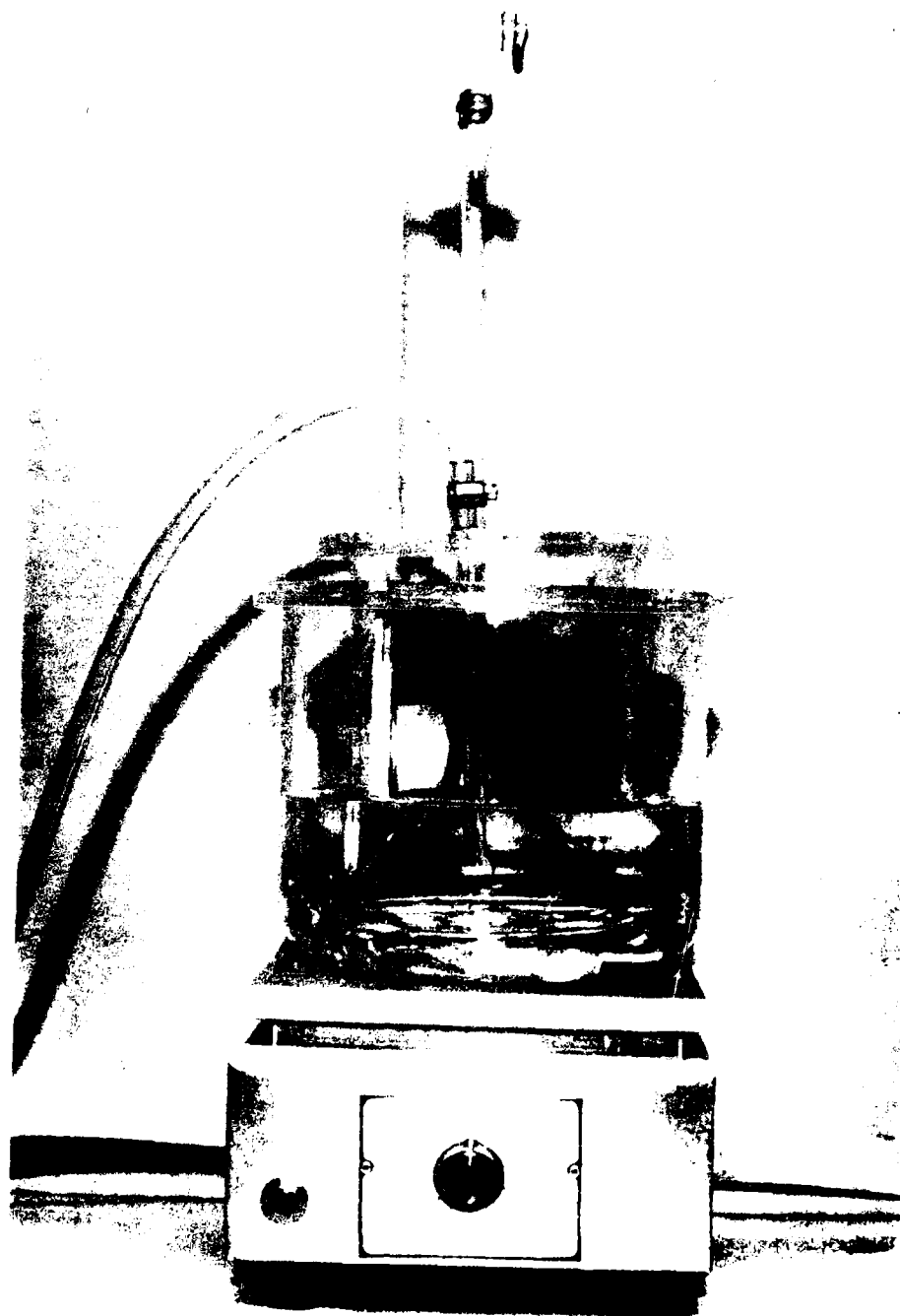


Fig. 1. Schematic diagram of the pump.

1. Drawing the silicone-oil up the entire length of the calibrated burette.
2. Placing the fritted-disc bubbler under the funnel and bubbling enough hydrogen into the burette to lower the meniscus to the calibrated portion of the burette.

Tests may be run until the meniscus comes to within approximately 3 inches of the silicone-oil bath level. At this point the above procedure must be used to establish a new initial hydrogen level because of the influence of the elevated temperature of the bath on the volume of the collected hydrogen.

#### Materials and Procedure

Initially, specimens were produced by welding HY-130, a high-strength low-alloy steel, with E14018 SMAW coated electrodes. Later investigations utilized a Russian pipeline steel 15Г2АФΔ (referred to as Steel 15 hereafter) as the base metal which was welded with either E7018 or E6010 SMAW coated electrodes. The chemical composition and mechanical properties of the materials used in this investigation are presented in Table 17 and 18, respectively.

Essentially, the same preparation and welding procedure were used for all welds. Initially, the base metal was machined into hydrogen-determination specimens with dimensions 5/8 x 5/8 x 1/4 inches (15.9 x 15.9 x 6.3 mm) in

TABLE 17

## CHEMICAL COMPOSITIONS OF MATERIAL USED IN THE RPI SILICONE-OIL INVESTIGATION

<u>MATERIAL</u>	<u>CONDITION</u>	<u>C</u>	<u>Mn</u>	<u>P</u>	<u>S</u>	<u>Si</u>	<u>NI</u>	<u>Cr</u>	<u>Mo</u>	<u>V</u>	<u>Ti</u>	<u>Al</u>	<u>Cu</u>
HY-130	2" Plate	0.100	0.77	0.005	0.003	0.200	4.92	0.560	0.052	0.060	0.01	0.026	--
15T2AØA	5/8" Plate	0.131	1.14	0.018	0.030	0.048	0.084	0.147	0.005	0.095	--	--	0.181
E14018 *	3/16" SMAW Electrodes	0.066	0.96	0.004	0.004	0.370	3.53	0.460	0.780	0.010	--	--	--
E7018 *	3/16" SMAW Electrodes	0.070	0.90	0.011	0.015	0.500	--	--	--	--	--	--	--
E6010 *	3/16" SMAW Electrodes	0.060	0.30	0.016	0.029	0.150	--	--	--	--	--	--	--

\*As-deposited



TABLE 18

## MECHANICAL PROPERTIES OF MATERIALS USED

<u>MATERIAL</u>	<u>Y.S.</u> <u>(KSI)</u>	<u>T.S.</u> <u>(KSI)</u>	<u>% ELONGATION</u> <u>(2" Gage Length)</u>
HY-130	136	147	19
15F2AΦΔ	60	78	19
E14018 <sup>*</sup>	141	147	18
E7018 <sup>*</sup>	73	84	30
E6010 <sup>*</sup>	55	65	25

Note: Weld Metal Properties for 43KJ/in Heat Input

\* Typical values for this material taken from producer's literature.

compliance with the BWRA/IIW specifications. All surfaces were ground flat and polished with 320-grit SiC paper. The initial weights of the polished specimens were recorded. Run-on and run-off tabs were machined and ground flat to dimensions  $5/8 \times 1\ 1/2 \times 1\ 1/2$  inches (15.9 x 38.3 x 38.3 mm).

Several polished specimens were positioned between the run-on and run-off tabs and loaded into the welding fixture, as illustrated in Figure 19. The entire assembly was degreased with acetone and demagnetized. Figure 20 shows the semi-automatic stickfeeder which was used to deposit the shielded metal arc (SMA) weld beads at  $\sim 30$  KJ/in (1180 J/mm) heat input. Table 19 summarizes the welding conditions employed. Within 15 seconds after extinguishing the arc, the welded specimen block was quenched in an agitated dry ice and alcohol bath at  $-70^{\circ}\text{C}$  ( $-94^{\circ}\text{F}$ ). Then, the specimens were mechanically separated and stored individually in liquid nitrogen at  $-196^{\circ}\text{C}$  ( $-320^{\circ}\text{F}$ ). At no time during the mechanical-separation procedure were the specimens removed from the dry ice and alcohol bath for more than 10 seconds, as specified by the BWRA/IIW procedure (Ref.1).

Prior to testing, the specimens were washed and dried according to the following 3-step procedure established by the BWRA:

1. Rinse in pure ethyl alcohol for 3-5 seconds.

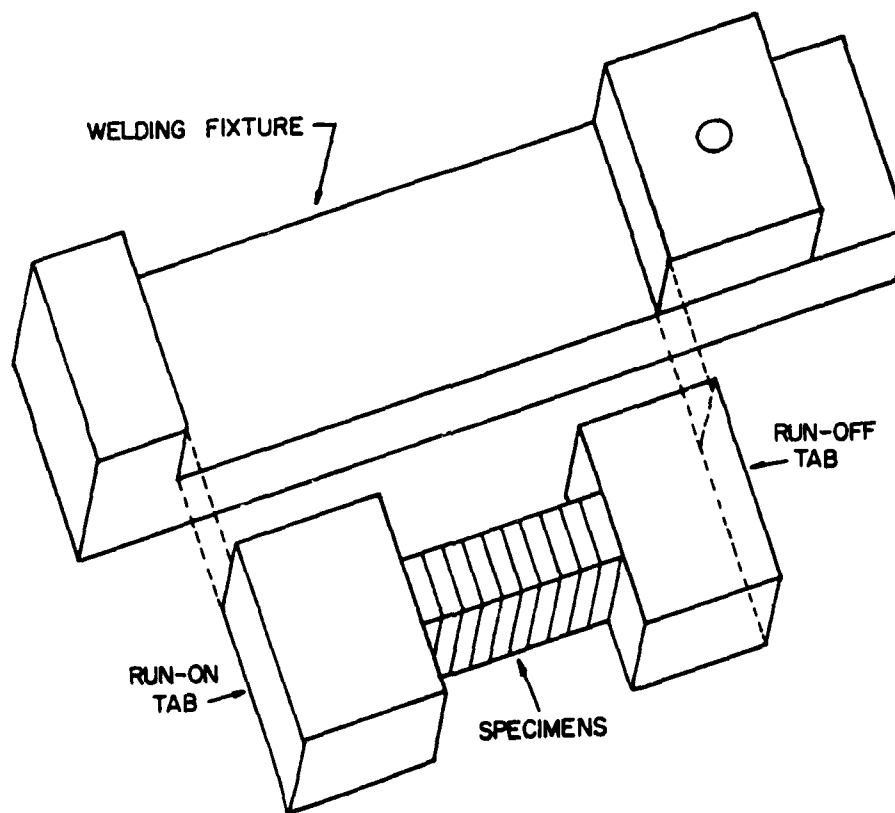


Figure 19. Schematic Illustration of the Welding Fixture and Specimen Arrangement.

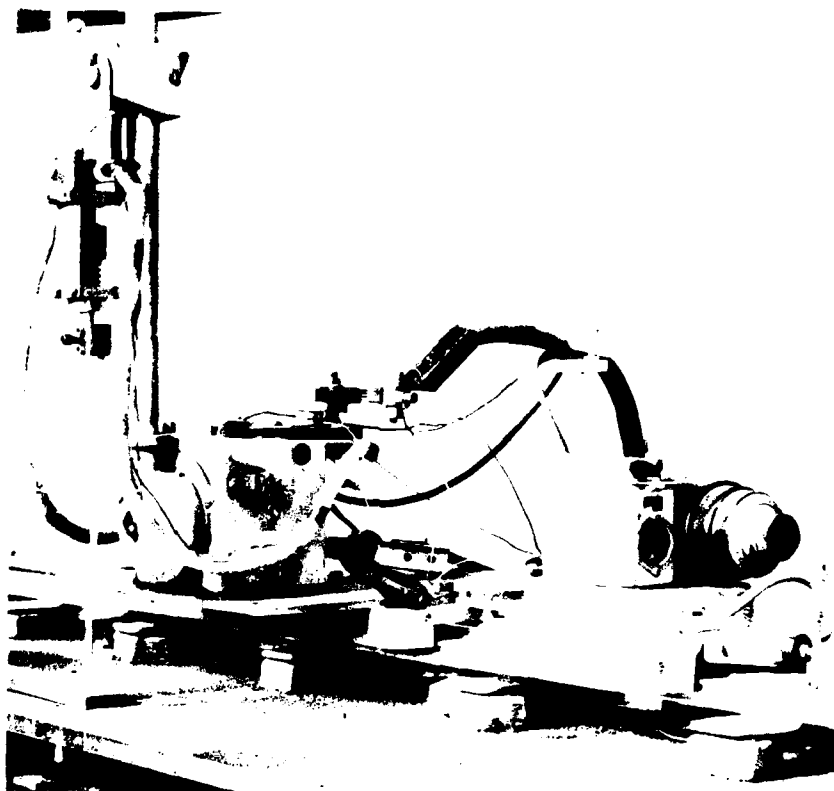


Figure 20. Semi-Automatic Stickfeeder Unit for Shielded Metal Arc Welding (SMAW).

TABLE 19

## Summary of Welding Conditions

<u>Electrode</u>	<u>Arc Voltage</u>	<u>Arc Current</u>	<u>Travel Speed</u>	<u>Energy Input</u>	<u>Condition of Electrode</u>
E14018	24V	160A	7.8 ipm	30 KJ/in	As-received
E14018	24V	160A	7.8 ipm	30 KJ/in	Coating Contaminated with Water
E7018	24V	160A	7.3 ipm	31 KJ/in	As-received
E6010	27V	140A	7.3 ipm	31 KJ/in	As-received

2. Rinse in anhydrous ethyl ether for 3-5 seconds.
3. Dry with a blast of low-dew-point argon gas for 20-30 seconds.

The total time of the wash is specified not to exceed 60 seconds. This washing procedure removes surface contaminants which could lead to inaccurate analysis of hydrogen content. After completion of a hydrogen analysis, the specimen was reweighed and a photomicrograph of its cross-section was taken.

The position of the hydrogen meniscus before and after testing determines the change in volume,  $\Delta V$ , of evolved hydrogen in cc. By use of the following equation,  $\Delta V$  is converted into ppm of hydrogen in weld metal at STP:

$$\text{PPM} = \Delta V \frac{273}{T} \frac{P}{29.92} \frac{90}{W}$$

where T is the temperature of the burette at the collection point, °K, P is atmospheric pressure (inches of Hg), W is the weight of the deposited weld metal (grams), and 90 is a conversion factor to convert the results from cc/gm to ppm of deposited weld metal.

The data for both the BWRA/IIW and the RPI Silicone-Oil methods are presented in units of ppm of hydrogen in the deposited weld metal,  $\text{ppm}_d$ , and ppm of hydrogen in the fusion zone metal,  $\text{ppm}_c$ . The use of these units requires the determination of the weight of the deposited weld metal,  $\Delta W_d$ , and that of the fusion zone which can be

approximated by the weight of the composition zone,  $W_C$ . The weight of the deposited weld metal,  $\Delta W_d$ , is determined by subtracting the initial (before-welding) weight of the specimen from the final (after-welding) weight of the specimen. On the other hand, the total weight of the composite zone of the weld is determined from planimeter measurements on a photomacrograph of:

1. The total area of the specimen, including the weld,  $A_T$ .
2. The area of the composite zone,  $A_C$ .

By using the final weight,  $W_F$ , and a simple ratio of areas, the weight of the composite zone,  $W_C$ , is determined:

$$W_C = \frac{A_C W_F}{A_T}$$

Calculations for the BWRA/IIW and the RPI Silicone-Oil Extraction techniques were performed utilizing both  $\Delta W_d$  and  $W_C$  to express the diffusible hydrogen contents in terms of  $\text{ppm}_d$  and  $\text{ppm}_C$ , respectively.

#### RESULTS AND DISCUSSION

Diffusible hydrogen content of HY-130 and Soviet Steel 15Г2АΦΔ weldments, as determined utilizing both the BWRA/IIW and RPI Silicone-Oil Extraction methods, are presented and discussed in the following.

## Determination of Diffusible-Hydrogen Content in HY130 Weldments

Table 20 shows typical data for low- and high-hydrogen welds in HY-130. These welds were deposited utilizing E14018 SMAW electrodes. The two levels of hydrogen content were achieved by using the electrodes in the as-received condition (low-range, approximately 2 ppm) or by soaking the electrodes in water for a minimum of 24 hours prior to welding (high-range, approximately 30 ppm). The welding conditions were previously noted in Table 19.

Note in Table 20 that only one determination of hydrogen content in each weld was made using the BWRA/IIW technique. This resulted from problems which were encountered in maintaining the BWRA/IIW apparatus in working condition. Approximately once every 8 tests, the BWRA/IIW apparatus experienced either a catastrophic fracture or an inability to hold vacuum for the required 72-hour test period. These failures resulted in significant loss of time for repairs and a loss of test results. It was determined that these failures resulted from scoring of the inner wall of the glass tubing by HY-130 steel specimens, which ultimately initiated cracking. Because of the difficulty in maintaining the BWRA/IIW apparatus in working condition, results in this section were limited to a comparison of four RPI diffusible-hydrogen determinations with only one BWRA/IIW determination for each weld.

Porosity was discovered in approximately 80-90% of the HY-130 welds which contained a high-hydrogen content.



TABLE 20

TYPICAL DATA FOR A LOW- AND A HIGH-HYDROGEN WELD  
IN HY-130

Spec#	Hydrogen Evolved(cc)	$\Delta W_d$ (g)	ppm <sub>d</sub>	$W_c$	ppm <sub>c</sub>
6J	0.020	0.6830	2.4	1.0820	1.5
*7J	0.060	0.9114	2.8	1.5132	1.7
8J	0.020	1.4389	1.2	2.5004	0.7
9J	0.020	0.8729	1.9	1.7593	0.9
10J	0.015	0.5627	2.2	1.2393	1.0
Mean Value, $\bar{x}$ = 2.1				$\bar{x}$ = 1.2	
Standard Deviation, $s$ = 0.6				$s$ = 0.4	
*1G	0.480	0.7070	31.6	1.8230	12.3
2G	0.385	1.2304	25.4	2.4756	12.6
3G	0.315	0.7909	32.7	1.6092	16.1
4G	0.305	0.7813	32.0	1.7144	14.6
5G	0.380	1.0872	28.4	1.9383	15.9
Mean Value, $\bar{x}$ = 30.0				$\bar{x}$ = 14.3	
Standard Deviation, $s$ = 3.1				$s$ = 1.8	

\* Tested By BWRA/IIW Method

Figure 21 is a photomacrograph of a specimen with a 18.6 ppm<sub>d</sub> hydrogen content which exhibits porosity. It has been demonstrated by Moreton, et al. (Ref.16), and confirmed by Savage, et al. (Ref.17), that hydrogen diffuses into the porosity voids where it reassociates into molecular form. Therefore, in view of the extreme amount of porosity encountered in HY-130 welds, the accuracy of the measured values of hydrogen concentration should be questioned.

Figures 22 and 23 show the correlation between the results of the RPI and BWRA/IIW methods for determining the diffusible hydrogen content of several HY-130 welds. The results are expressed in ppm of hydrogen based on the weight of the deposited metal,  $\Delta W_d$ , in Figure 22, and on the composite-zone weight,  $W_c$ , in Figure 23. The analysis based on deposited metal weight has been termed ppm<sub>d</sub>, whereas the analysis based on the composite-zone weight has been termed ppm<sub>c</sub>. Because difficulties were experienced with the BWRA/IIW apparatus and the extreme porosity was encountered in the welds, the results of these tests were inconclusive. Therefore, further testing was needed to establish a relationship.

#### Determination of Diffusible-Hydrogen Content in Soviet Steel 15Г2АФΔ (Steel 15) Weldments

Correlation between the BWRA/IIW and RPI Methods. In order to decrease the failure rate of the hydrogen deter-

AD-A094 219

RENSSELAER POLYTECHNIC INST TROY N Y  
DEVELOPMENT AND QUALIFICATION OF METHODS FOR THE DETERMINATION --ETC(U)  
SEP 80 W F SAVAGE, E F NIPPES

N00014-75-C-0944

NL

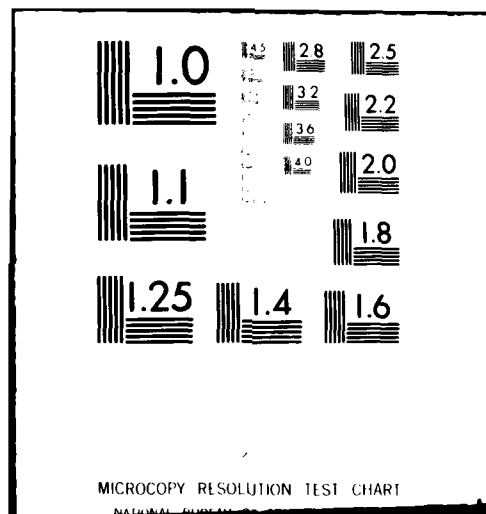
UNCLASSIFIED

2 1/2 2

200 1/2 1/4



END  
DATE  
FILMED  
2-81  
DTIC



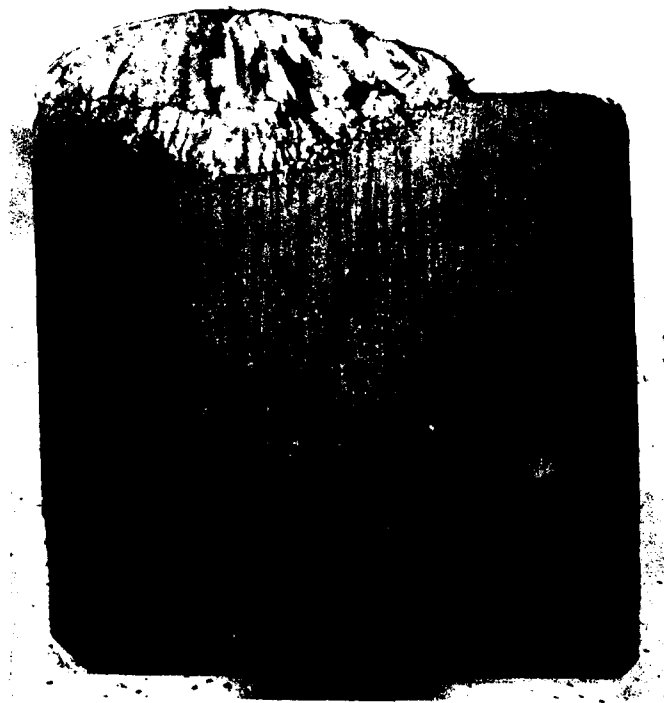


Figure 21. Photomacrograph of a High-Hydrogen Weld  
Which Exhibits Porosity ( $\text{ppm}_d = 18.6$ ), 5X.

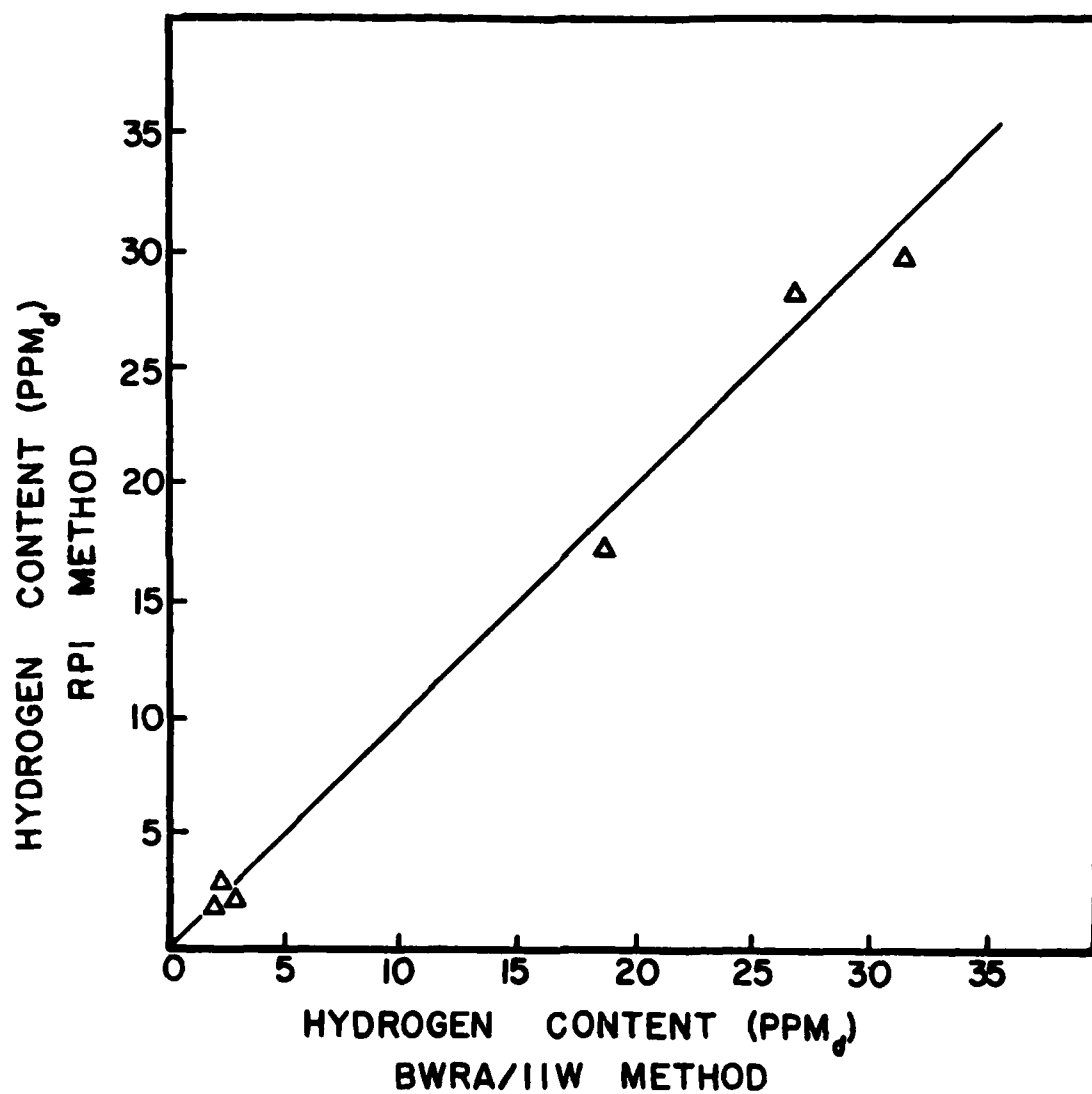


Figure 22. Correlation Between the RPI and BWRA/IIW Methods in ppm<sub>d</sub> of Diffusible Hydrogen in E14018/HY-130 Weldments, Utilizing Deposited-Metal Weight,  $\Delta W_d$ .

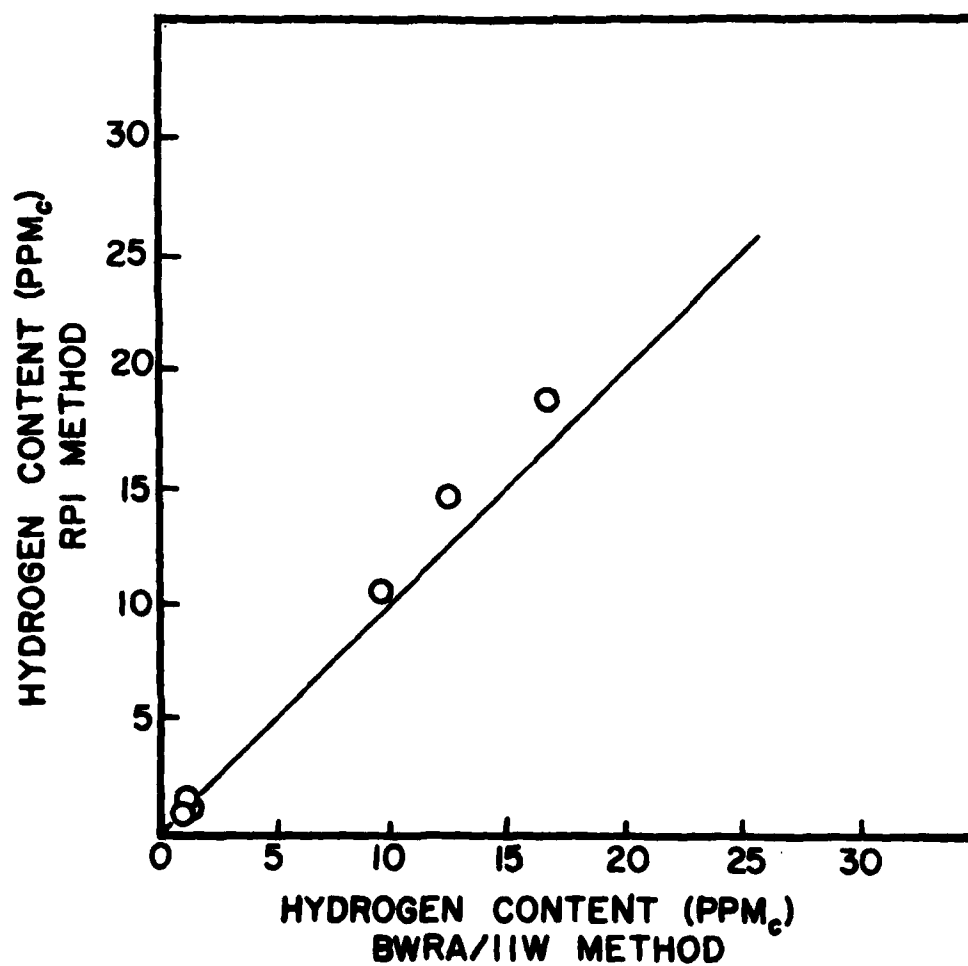


Figure 23. Correlation Between the RPI and BWRA/IIW Methods in ppm<sub>c</sub> of Diffusible Hydrogen in E14018/HY-130 Weldments, Utilizing Composite-Zone Weight, W<sub>c</sub>.

minations utilizing the BWRA/IIW apparatus, a softer steel, Steel 15, was used as the base metal, porosity was reduced by replacing the E14018 electrodes with two SMAW electrodes, E7018 and E6010, which produced low- and high-hydrogen levels, respectively. Utilizing this softer steel, two BWRA/IIW hydrogen determinations were obtained from each weld run. For both low- and high-hydrogen content welds, porosity was virtually eliminated.

Figures 24 and 25 show comparisons between the hydrogen contents determined by the RPI and BWRA/IIW methods based on  $\text{ppm}_d$  and  $\text{ppm}_c$ , respectively. Note that in both cases there is good correlation between the two methods. In contrast to most published findings (Ref.15), utilization of the composite-zone weight results in significantly better correlation than that of the deposited-metal weight. This is evidenced by the correlation coefficients,  $R^2=0.93$  and  $R^2=0.74$ , for the calculations utilizing  $W_c$  and  $\Delta W_d$ , respectively. Research by Tsunetomi, et al. (Ref.10), has demonstrated that the entire molten weld pool, a mixture of base and deposited metal, acts as the sink for diffusible hydrogen. Therefore, it is appropriate to use the composite-zone weight (the solidified weld pool) for calculating the diffusible-hydrogen contents.

Liberation of gas from the entire fusion zone of the weld, which was observed during testing in the RPI method, confirmed that the entire weld pool is a sink for diffusible hydrogen during welding.



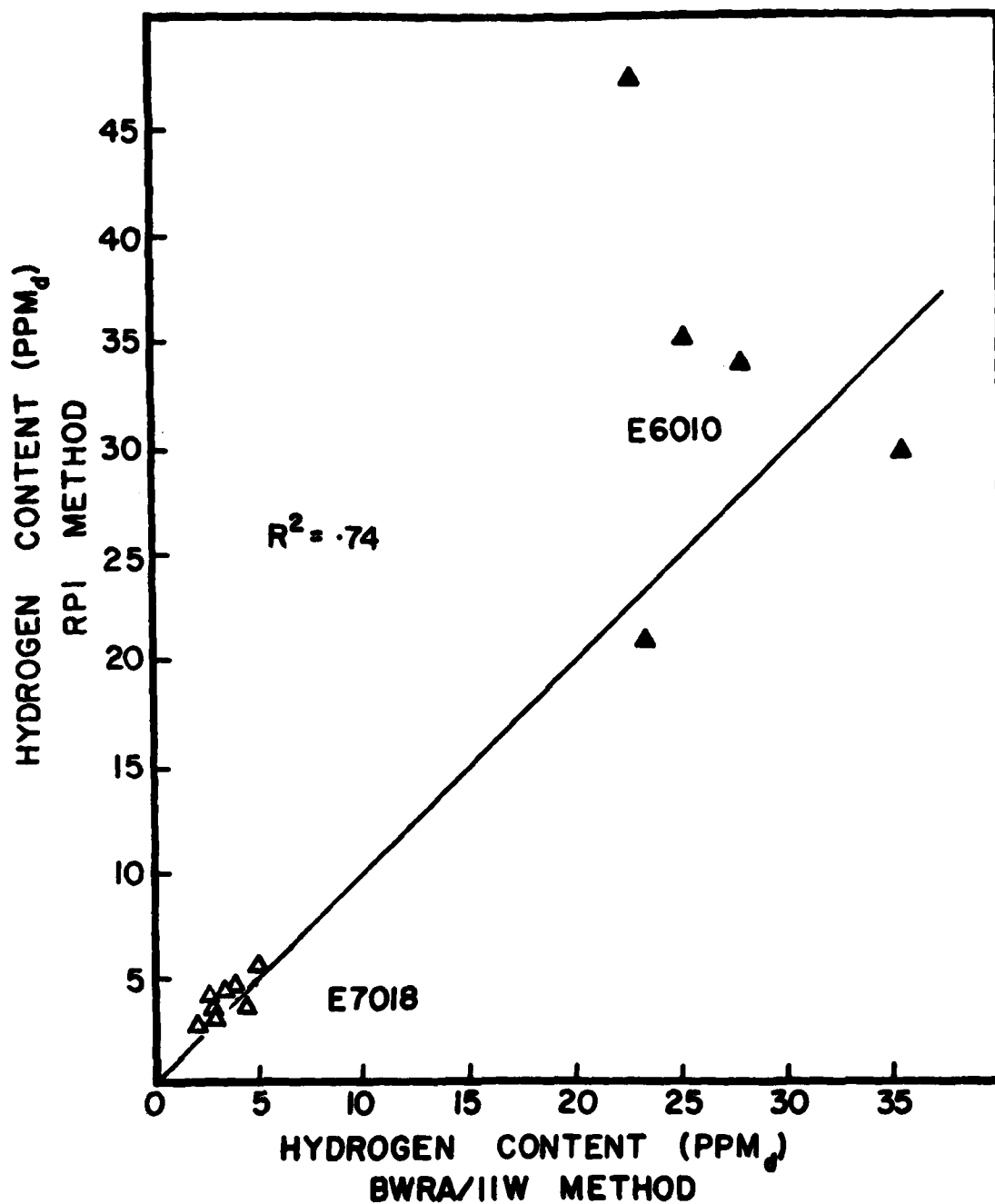


Figure 24. Correlation Between the RPI and BWRA/IIW Methods in ppm<sub>d</sub> of Diffusible Hydrogen in Steel 15 Weldments, Utilizing Deposited-Metal Weight,  $\Delta W_d$ .

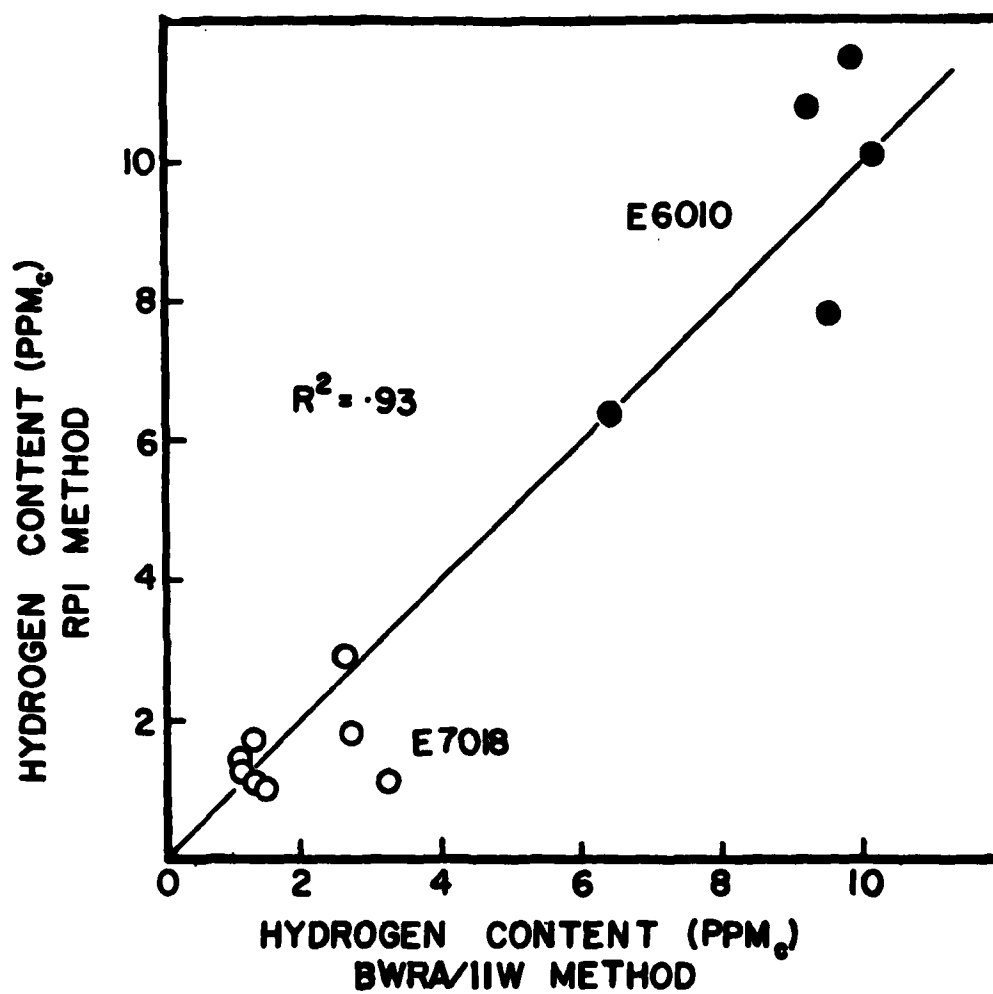


Figure 25. Correlation Between the RPI and BWRA/IIW Methods in ppm<sub>c</sub> of Diffusible Hydrogen in Steel 15 Weldments, Utilizing Composite-Zone Weight,  $W_c$ .

Table 21 shows typical diffusible-hydrogen content data for a low- and a high-hydrogen weld in Steel 15. Calculations of hydrogen content expressed in  $\text{ppm}_C$  show much greater consistency than those expressed in  $\text{ppm}_D$ . This is exemplified by their standard deviations:  $0.8 \text{ ppm}_C$  vs.  $5.6 \text{ ppm}_D$  for the high-hydrogen weld and  $0.3 \text{ ppm}_C$  vs.  $1.3 \text{ ppm}_D$  for the low-hydrogen weld.

Data from an additional low-hydrogen weld are presented in Table 22. Note that Sample 23 has a negative  $\Delta W_D$  value, although weld metal was deposited, as shown in Figure 26. The mechanical separation of Sample 23 produced a specimen surface which was not planar, and a fracture surface which was not parallel to the original specimen surface. As a result, the thickness of the specimen in the fused region was less than the original thickness of the specimen. This condition, in conjunction with the small amount of weld reinforcement, resulted in the negative value of  $\Delta W_D$  shown in Table 22. However, the value of the hydrogen content of this specimen, obtained by utilizing the composite-zone weight, is comparable with those obtained from other specimens in this weld.

#### Influence of Hydrogen Content on Extraction Time

Figure 27 shows the extraction volume of diffusible hydrogen as a function of time for two specimens: Sample 1810 with a high-hydrogen content ( $6.5 \text{ ppm}_C$ ) and Sample 46 with a low-hydrogen content ( $0.9 \text{ ppm}_C$ ). Note that for both

TABLE 21

TYPICAL DATA FOR A LOW- AND A HIGH-HYDROGEN WELD  
IN STEEL 15

Spec#	Hydrogen Evolved(cc)	$\Delta W_d$ (g)	ppm <sub>d</sub>	$W_c$ (g)	ppm <sub>c</sub>
46	0.015	0.5465	2.3	1.4150	0.9
*47	0.090	0.7336	3.7	1.5844	1.7
*48	0.100	1.3045	2.3	2.3103	1.3
49	0.020	0.7515	2.2	1.6072	1.0
410	0.020	0.3321	5.1	1.5756	1.1
Mean Value, $\bar{x}$ = 3.1					$\bar{x}$ = 1.2
Standard Deviation, s = 1.3					s = 0.3
181	0.120	0.5139	19.6	1.6705	6.0
182	0.120	0.2739	35.2	1.2563	7.7
183	0.095	0.4105	19.4	1.3888	5.7
184	0.110	0.5459	16.9	1.5421	6.0
*185	0.170	0.3183	21.8	1.2977	5.3
*186	0.220	0.3796	25.1	1.2764	7.5
187	0.080	0.4041	16.6	1.2474	5.4
188	0.100	0.4738	17.6	1.2582	6.6
189	0.100	0.3614	23.2	1.2065	6.9
1810	0.145	0.6477	18.8	1.8672	6.5
Mean Value, $\bar{x}$ = 21.4					$\bar{x}$ = 6.4
Standard Deviation, s = 5.6					s = 0.8

\* Tested By BWRA/IIW Method

TABLE 22

## DATA FOR A LOW-HYDROGEN WELD IN STEEL 15

<u>Spec#</u>	<u>Hydrogen Evolved(cc)</u>	<u><math>\Delta W_d</math>(g)</u>	<u>ppm<sub>d</sub></u>	<u>W<sub>c</sub></u>	<u>ppm<sub>c</sub></u>
21	0.020	0.3230	5.2	1.0502	1.6
*22	0.020	0.5245	2.3	1.3066	0.9
23	0.015	-0.0033	---	1.3986	1.2
*24	0.050	0.6183	4.1	2.0576	1.2

Mean Value,  $\bar{X}$  = 3.9                       $\bar{x}$  = 1.2  
Standard Deviation, s = 2.1                      s = 0.3

\* Tested by BWRA/IIW Method.



Figure 26. Sample 23 Which Exhibits a Negative  $\Delta w_d$ , 5X.

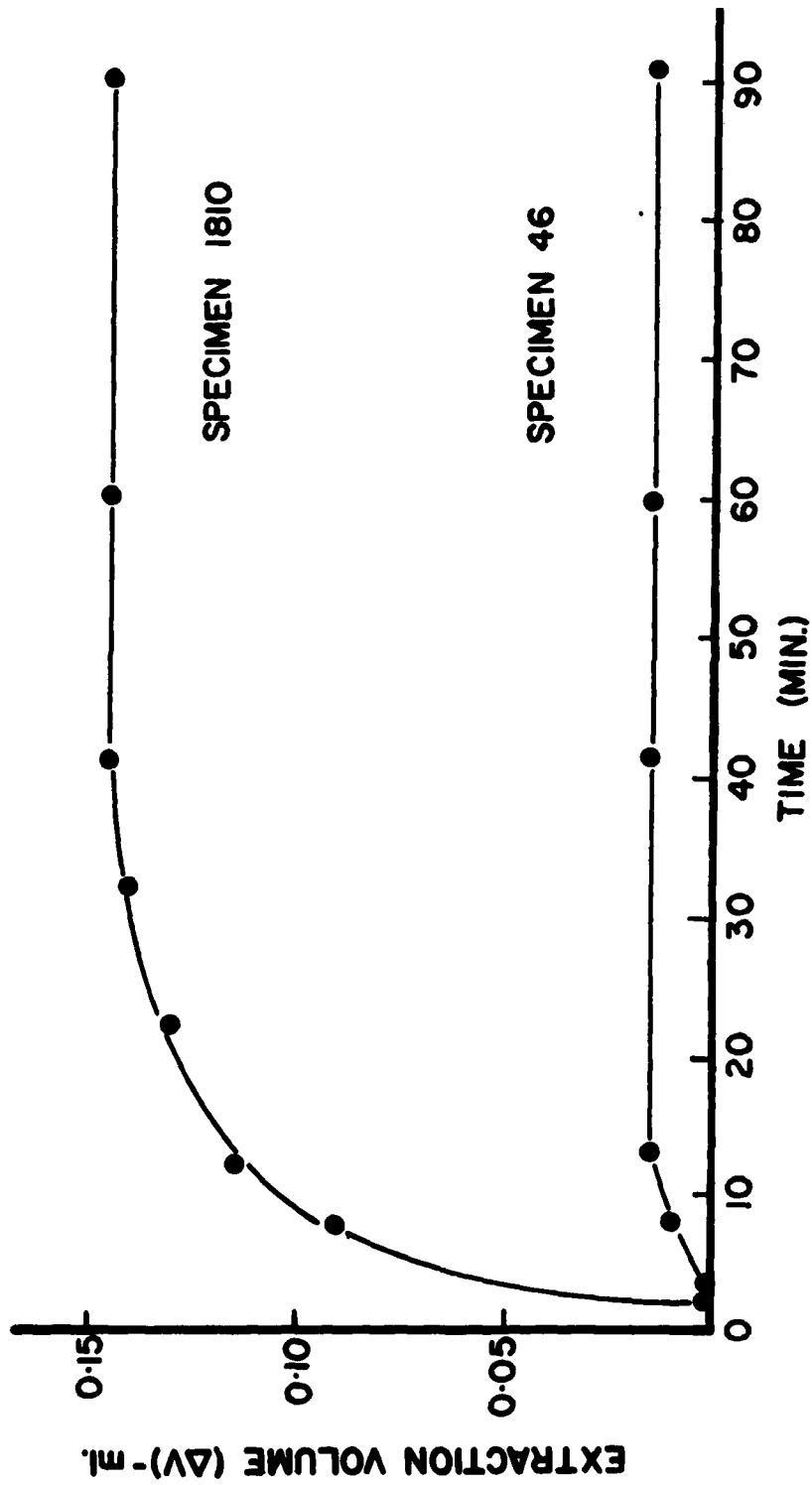


Figure 27. Plot of Extraction Volume of Diffusible Hydrogen ( $\Delta V$ ) vs. Time For a Low- and High-Hydrogen Weld.

specimens, there is an incubation time before evolution begins. This time delay, which is necessary for hydrogen diffusion to the sample surface, is a characteristic of hydrogen-extraction methods. Also, it is to be noted that the extraction curves for both samples level off well before the recommended test time of 90 minutes.

#### Advantages of the RPI Silicone-Oil Extraction Method

Hydrogen determinations utilizing the RPI method have shown a direct correlation with those utilizing the BWRA/IIW technique. In addition, the RPI Silicone-Oil Extraction Method exhibits several important advantages over the BWRA/IIW technique:

1. Short test time of 90 minutes.
2. Vacuum is not necessary.
3. Hazardous mercury is not required.
4. Adaptable to large specimen sizes.
5. Non-magnetic specimens may be used.
6. Simple and inexpensive test equipment.
7. The location time which gas evolves from the specimen may be observed.

#### SUMMARY

The RPI Silicone-Oil Extraction Method is a reliable, rapid, and inexpensive technique for the determination of



diffusible hydrogen contents in weldments.

Diffusible hydrogen contents of weld specimens determined utilizing the RPI method were comparable to the results of BWRA/IIW tests of other specimens from the same weld. The use of composite zone weight,  $W_c$ , in place of the deposited weld metal weight,  $\Delta W_d$ , in determining the diffusible-hydrogen content yields better consistency of results for both the RPI and BWRA/IIW methods. In addition, utilization of the composite zone-weight in computing the diffusible-hydrogen content resulted in better correlation between the RPI and BWRA/IIW extraction techniques.

## GENERAL CONCLUSIONS

### I. Mass-Spectrometer Hot-Extraction Method.

1. A decanting method has been devised to obtain weld-metal samples for hydrogen analysis.
2. Water, carbon tetrachloride, and liquid nitrogen were not suitable quenchants for the decanted weld-metal samples.
3. When water was used as a quenchant, the liquid-metal decant samples dissociated the surrounding water into atomic hydrogen. The adsorption of this hydrogen increased the amount of diffusible hydrogen in the decant specimen by a factor of three.
4. When either carbon tetrachloride or liquid nitrogen was used as a quenchant, the rates of cooling were not adequate to prevent the diffusion of hydrogen from the decant specimens. As a result, the measured amount of diffusible hydrogen in the decant was reduced by a factor of two.
5. If a suitable quenching procedure were developed, the mass-spectrometer extraction method could be used to measure the diffusible and total hydrogen contents of weld-metal specimens.

## II. Modified Barnacle Cell Method.

1. Because preliminary testing indicated difficulties with the Barnacle Cell in its original, clamp-on configuration, the cell was modified to permit complete immersion of the specimen.
2. The driving electrode in the Barnacle Cell was replaced with an electronic potentiostat.
3. Extraction transients from standard, welded BWRA/IIW specimens could not be related to the Gileadi diffusion solution for extraction of hydrogen from rectangular specimens. The additional anodic area, the cylindrical geometry of the weld metal, and the non-uniform hydrogen content of the weldment invalidated the application of Gileadi's diffusion solution to the BWRA/IIW specimens.
4. The Barnacle Cell current-time transients from weld-decant specimens did not match the Fourier transform solution for diffusion from a sphere. The decanted weld specimens contained extensive cracking which resulted either directly from the quench, or from hydrogen embrittlement. Decanted weld-metal specimens could not be tested, successfully, because the cracks provided additional, non-spherical, anodic area for the extraction of hydrogen from the specimens.
5. In the modified Barnacle Cell, the measured current-time transients from specimens of known initial

hydrogen content could not be matched to the spherical diffusion solution, over the full period of observation from 30 to 4000 secs. However, extraction transients from hydrogen-charged steel shot were related successfully to transients generated from the Fourier transform spherical diffusion solution in the time interval 1200 to 2000 secs.

6. Current-time transients obtained from uncharged and vacuum-degassed specimens were negligible. These results indicate that competing reactions in the Barnacle Cell do not have a significant effect on the measured extraction currents.
7. Mathematically, the solutions to the diffusion equation are sensitive to the value of hydrogen diffusivity,  $D$ , that is selected.
8. Therefore, the modified Barnacle Cell cannot be used to determine accurately the diffusible hydrogen content in weldments because accurate diffusivity values are not known, or are difficult to determine.

### III. RPI Silicone-Oil Extraction Method.

1. The RPI Silicone-Oil Extraction Method is a reliable, rapid and inexpensive technique for the determination of diffusible-hydrogen content in weldments.

2. The use of the composite-zone weight, rather than the deposited weld metal weight, in determining the diffusible-hydrogen content yields a better consistency of results for both the RPI and BWRA/IIW methods.
3. The use of the composite-zone weight in calculating the diffusible-hydrogen content yields a better correlation between the results of the RPI and the BWRA/IIW extraction techniques.

## REFERENCES

1. Coe, F. R.; "Hydrogen in Weld Metal," British Welding Research Association Bulletin, Vol. 8, (1967).
2. Jenkins, N. and Coe, F. R.; "Hydrogen Analysis at BWRA; the BWRA Apparatus," British Welding Research Association Bulletin, Vol. 7, (1966).
3. Boillot, P. and Hanin, M.; "Fast Determination of Hydrogen in Steels and Non-ferrous Metals," Institut de Recherches de la Siderurgie Francaise (IRSID), Paris, France, Re 184 bis (1973).
4. Pokhodnya, I. K. and Paltsevich, A. P.; "Chromatographic Method for Estimating an Amount of Diffusion Hydrogen in Welds," E. O. Paton Electric Welding Institute of the Academy of Sciences of the Ukrainian SSR, (1979).
5. Berman, D. A., Beck, W., and DeLuccia, J. J.; "The Determination of Hydrogen in High Strength Steel Structures by an Electrochemical Technique," Hydrogen in Metals, American Society For Metals, Seven Springs Conference Proceedings, Champion, PA, 1973, p. 595.
6. Berman, D. A.; "Development of an in-situ Electrochemical Method to Determine Embrittling Hydrogen in Steel Weldments and Structures (Barnacle Electrode), Report No. NADC-74219-30, Naval Air Development Center, Warminster, PA, 1974.
7. Berman, D. A., Beck, W., and DeLuccia, J. J.; "Hydrogen in Metals," A.S.M. Materials and Metalworking Technology, Series No. 2, Bernstein, I. M. and Thompson, A. W. Editors, 595-607 (1974).
8. Berman, D. A.; "Indexing the Degree of Hydrogen Embrittlement of 4340 Steel Using the Barnacle Electrode, Report No. NADC-76359-30, Naval Air Development Center, Warminster, PA, 1976.
9. Berman, D. A., DeLuccia, J. J., and Mansfeld, F.; "Barnacle Electrode: New Tool for Measuring Hydrogen in High Strength Steels," Metal Progress, 115(5), 58-61, (1979).
10. Tsunetomi, E. and Murakami, S.; "Comparison Between IIW and JIS Procedures for Determination of Diffusible Hydrogen," International Institute of Welding, Document II-A-288-71, (1971).

11. Hudson, J. B. and Watters, R. L.; "The Monopole-A New Instrument for Measuring Partial Pressures," I.E.E.E. Transactions on Instrumentation and Measurement, Vol. IM-15, No.3, pp. 94-98 (1966).
12. Greene, N.; "Experimental Electrode Kinetics," Electrochemistry Laboratory Manual, Rensselaer Polytechnic Institute, Troy, NY, (1965).
13. Devanathan, M. and Stachurski, Z.; "The Adsorption and Diffusion of Electrolytic Hydrogen in Palladium," Proceedings of the Royal Society, Vol. A 270, London, p. 90, (1962).
14. Gileadi, E. and Bockris, J.; "Hydrogen Embrittlement Resulting from Corrosion, Cathodic Protection, and Electroplating," Final Report, U.S. Navy NAEC Contract No. N156-46659, The Electrochemistry Laboratory, University of Pennsylvania, Philadelphia, (1966).
15. Coe, F. R.; "Welding Steels Without Hydrogen Cracking," The Welding Institute, Cambridge, England, (1973).
16. Moreton, J., Coe, F. R., Boniszewski, T.; "Hydrogen Movement in Weld Metals," Metal Construction, 3(5), 185-187, (1971).
17. Savage, W. F., Nippes, E. F., and Silvia, A. J.; "Prevention of Hydrogen-Induced Cracking in HY-130 Weldments," Interim Technical Report, July 1, 1976 to June 30, 1977, Office of Naval Research Contract No. N00014-75-C-0944, NR 031-780, (1977).

END

DATE  
FILMED

2-81

DTIC